Professor Lidia Morawska
International Laboratory for Air Quality and Health
Queensland University of Technology
2 George Street, Brisbane QLD 4001 Australia
Email: l.morawska@qut.edu.au

5th July 2018

Natascha Töpfer
Copernicus Publications
Editorial Support
editorial@copernicus.org

Dear Natascha,

Submission of Revised Manuscript Number: acp-2018-189

Title: Differentiating between particle formation and growth events in an urban environment

Authors (names and email addresses):

Ms. Buddhi Pushpawela: buddhi.pushpawela@hdr.qut.edu.au
Dr. Rohan Jayaratne: r.jayaratne@qut.edu.au
Prof. Lidia Morawska: l.morawska@qut.edu.au

As requested, we have considered the comments of the three anonymous reviewers in detail and revised the paper accordingly.

I am submitting the following documents:

(1) Revised Manuscript

(2) Revised Manuscript with all changes indicated in Track Changes

(3) Detailed responses to Anonymous Reviewers 1, 2 and 3.

I hope you will find it acceptable for publication in ACP.

Please contact me at the email address below, should you have any further queries.

Yours sincerely,

Professor Lidia Morawska, PhD

Director
International Laboratory for Air Quality and Health
WHO CC for Air Quality and Health

Director - Australia
Australia – China Centre for Air Quality Science and Management
Queensland University of Technology
Phone: +61 7 3138 2616
Fax: +61 7 3138 9079
E-mail: l.morawska@qut.edu.au

Response to Anonymous Referee #1

Overall Comment

The manuscript describes the difference between growth pattern during two main types of conditions:

(1) Right after a NPF event

(2) without a NPF

This idea is actually interesting to consider.

Comment 1

In case this will be published in ACPD, I would love the authors to make a more extensive literature review abut NPF studies in the urban atmospheres such as that reported in Japan, China, and different parts in the EU (particularly in Scandinavian countries and central Europe).

Response 1

While there are many papers reporting NPF in urban environments, there are a limited number of papers reporting night time NPF events. In Table 1, we have listed only those studies that have reported occurrence rates of NPF events BOTH during the day time and the night time.

Comment 2

Another important point that needs to be also resolved is the night tie events and how the authors considered the start and end of night time. The authors took a fixed time for both sunrise and sunset. I would rather see this analysis to into account the real sun rise and sunset time.

Response 2

The method of estimating the start times of NPF events is as stated in Lines 141-146:

"Every NPF event was characterised by a sharp increase of the PNC in the intermediate size range from 2.0-7.0 nm. This observation has been used to determine the starting time of an NPF event (Leino et al., 2016). Similarly, in the present study, the starting time of a strong NPF event was determined by noting the time of first occurrence of dN/dt > 10,000 $cm^{-3}h^{-1}$. The starting time of a weak NPF event was determined by noting the time of first occurrence of dN/dt > 5000 $cm^{-3}h^{-1}$. N is the number of particles in the size range 2.0-10 nm".

In this paper, we did not consider the end times of NPF events.

We considered the real sunrise and sunset times and the results are shown in the two figures below. Figure 1(a) shows the 'daytime' events with time after sunrise shown on the x-axis.

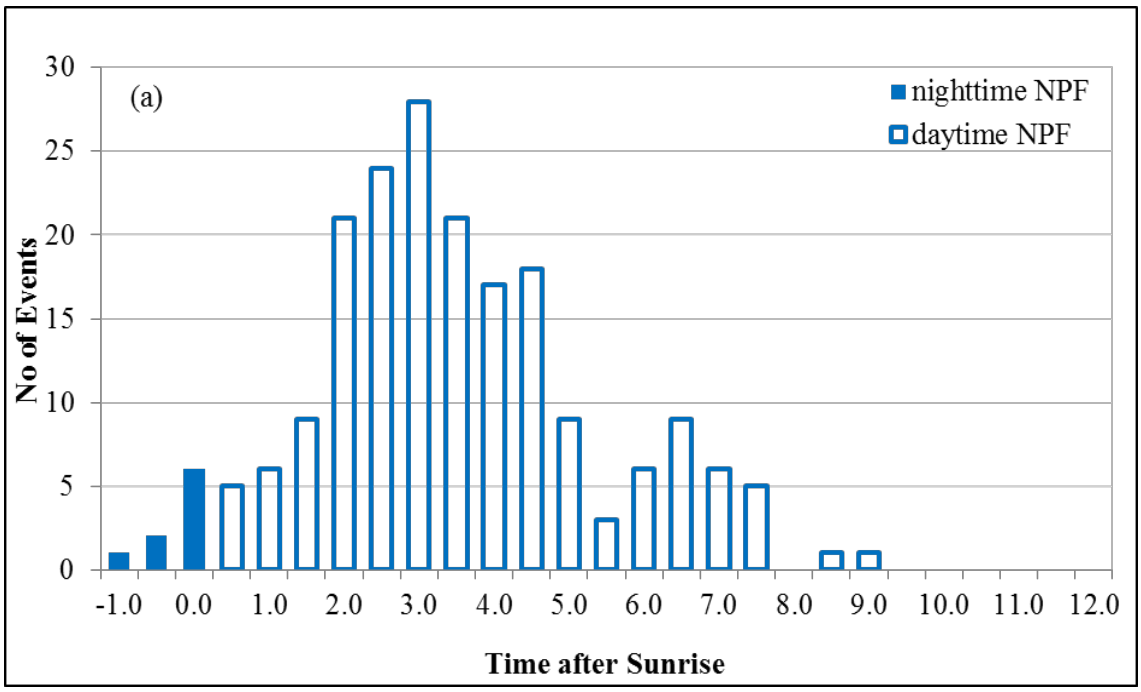

Figure 1(a): Distribution of start times of daytime NPF events as a function of time after sunrise.

The three bars on the extreme left correspond to times before sunrise. We have classified these as 'night time events'.

Figure 1(b) shows the 'night time' events with time after sunset shown on the x-axis.

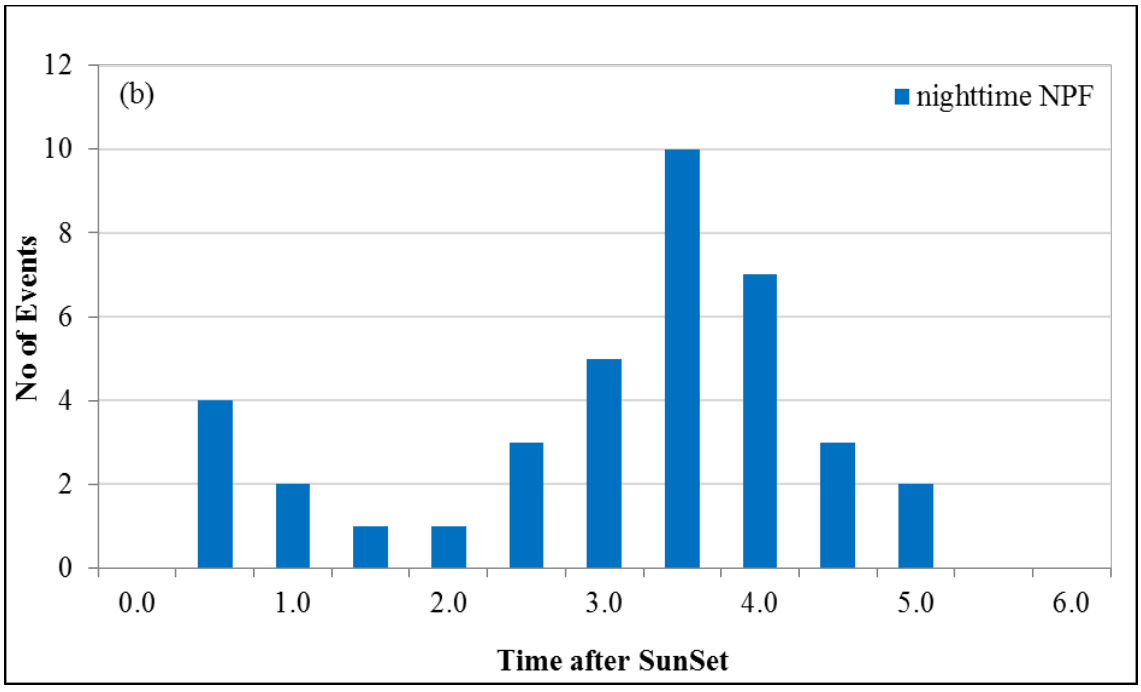

Figure 1(b): Distribution of start times of night time NPF events as a function of time after sunset.

We have deleted the original Figure 1(a) as suggested by Anonymous Referee #2 and replaced the original Figure 1(b) with these two new figures.

Replacing real time with times after sunrise and sunset introduces quite a few changes to the description. To accommodate this, we have included the following new text into the paper:

In Section 3.2, Lines 248-256:

"Figures 1 (a) and (b) shows the summary of starting times of all NPF events during the day time and night time, respectively, estimated by using the method described in Section 2.3.1. The histograms show the number of events observed in each 30 min period after sunrise and sunset, respectively. The times indicated on the x-axis refer to the end of each 30 min period. In Figure 1(a), the three bars at the extreme left correspond to times before sunrise. We have classified these as night time events. Both of these figures show that most NPF events (71%) began during the morning, with a high likelihood of occurrence between 2 and 4 hours after sunrise, corresponding to approximately between 8.00 am and 10.00 am".

And in Lines 262-264:

"The starting times of night time NPF events also showed a distinct trend with a peak likelihood between 3 and 4 hours after sunset, corresponding to approximately 8 and 9 pm".

And, in Section 474-477, Line (Summary and Conclusions):

"71% of NPF events occurred during the morning, with the highest probability of occurrence between 2 and 4 hours after sunrise, corresponding to approximately between 8.00 am and 10.00 am. Most of the night time events occurred between 3 and 4 hours after sunset, corresponding to approximately between 8.00 pm and 9:00 pm".

Response to Anonymous Referee #2

Overall Comments

This manuscript presents an analysis on new particle formation (NPF) and growth events based on extensive ambient measurements at an urban location. This is a valuable data set that should be published. However, in its current form the manuscript requires revisions, some of which can be considered substantial. My detailed comments in this regard are given below.

Comment 1

The last two paragraphs in section 3.4 give an impression that sub-10 nm particles might grow faster in this environment than larger particles. This is an interesting observation, if true. In most sites where ion spectrometers have been used for reported NPF studies, the particle growth rate was observed to increase from sub-3 nm sizes up to 10-20 nm. I would like to see a bit more discussion on this topic in this paper, including comparison to earlier studies.

Response 1

We have inserted the following text on section 3.4 Lines 333-349:

"Typically, the particle growth rates were high during the first few hours and then decreased to a few nanometres per hour within 3-4 hours after nucleation. Several studies have reported that the growth rate of particles in the size range 7-20 nm was greater than that in the smaller size range 3-7 nm (Backman et al., 2012; Gagne et al., 2011; Manninen et al., 2010; Yli Juuti et al., 2009). Manninen et al (2010) studied NPF events at 12 European sites and found that 9 out of the 12 sites showed this trend while at 3 sites the growth rate was greater in the smaller size range. They suggested that this size dependence was due to different condensing vapours participating in the growth of different sized particles depending on their saturation vapour pressures. For example, it is well known that sulfuric acid plays a dominant role in nucleation and the initial growth of particles during NPF while organics dominate the growth at larger sizes of 10-30 nm (Smith et al, 2008; Manninen et al., 2009; Yli-Juuti et al., 2011). Further evidence comes from the observation that the growth rate of the particles in the larger size range of 7-20 nm is enhanced during the summer when the concentration of biogenic volatile organic compounds in the atmosphere is greater (Yli-Juuti et al., 2011). Our observations of particle growth rates in the different size ranges agree with previous studies that have suggested that the dominant condensable vapour in Brisbane is probably sulfuric acid, with organics playing a secondary role (Crilley et al, 2014)".

Comment 2

I am surprised how the authors ended up in selecting the few short-term campaigns when discussing particle growth following NPF in section 3.6 (lines 322-328). Growth to larger sizes occurs very frequently in so-called regional NPF events and in many locations, newly-formed particles have been observed to grow up to sizes where they may act as cloud condensation nuclei (50-150 nm in diameter). So growth following NPF is a very common phenomenon. The authors should bring this up more clearly in that paragraph, now the reader easily get a wrong impression that growth to larger sizes is kind of a rare phenomenon.

Response 2

As stated in Section 2.1, *"The measurements were carried out during the three calendar years 2012, 2015 and 2017, yielding 485 complete days of data".* Figures 4 and 5 in Section 3.6 are just two examples of a few days each. They are not short-term campaigns.

We have modified the first sentence of this paragraph as follows , Lines 391-392:

"Continued growth of particles following NPF events is a common phenomenon and has been reported by several other researchers".

Comment 3

I am not comfortable with the last paragraph of section 3.6 (lines 343-358). By reading it, one easily gets an impression that water uptake alone might explain the observed particle growth at increasing RH. This is very unlikely to be the case. Firstly, comparison of the growing particles water uptake to that by NaCL is unfair, since the latter is perhaps the most hygroscopic material present in the ambient atmosphere, while ultrafine particles in an urban environment are (based on measurements in several sites) much less hygroscopic. However, high RH might favor particle growth due to other reasons: 1) heterogenous reactions taking place in the liquid phase of the growing particles, or 2) simply due to the fact that an increase in RH is often accompanied by a decrease in ambient temperature, which would favor the transport of any semi-volatile

compounds from the gas phase to these particles. I would recommend rewriting this

paragraph and removing Figure 7 altogether.

Response 3

We have removed Figure 7 along with its discussion, as suggested, and modified the text in this paragraph to accommodate the comments of the reviewer. It now reads as follows, Lines 413-435:

"It is well-known that relative humidity may favour particle growth in the atmosphere owing to several reasons. For example, atmospheric aerosol particles increase in size with relative humidity due to the uptake of water (Winkler, 1988). In addition, when the relative humidity increases, heterogeneous reactions can take place in the liquid phase of a growing particle while, if there is an accompanying drop in temperature, it would enhance the transport of semivolatile compounds from the gas phase on to the surface of the particles. Water uptake is caused by the deliquescence of soluble salts which form a solution when the solid compound is exposed to water vapour at sufficiently high vapour pressure. Several organic materials are also known to absorb water at high humidity which is more generally known as hygroscopicity. Sodium chloride (NaCl) has a deliquescence point of 76% relative humidity. At this point, a NaCl-bearing particle will deliquesce and become a solution of droplet with a well-defined spherical shape. The particle diameter does not change considerably as the relative humidity is increased from 0 to 74%, beyond which it can increase considerably. Close to the coast, sea-salt aerosols constitute a large proportion of the atmospheric particulate mass and NaCl is a major component. Many of the inorganic substances that readily absorb water, such as sea salt, ammonium salts and nitrates, are present in the Brisbane environment (Harrison, 2007). Therefore, it is not surprising that, in the present study, we observed that particle growth occurred on 7 out of 10 nights with high relative humidity".

Comment 4

In addition to the paragraphs mentioned above, there are many places in the text that

lack references, either totally or proper/fresh ones: 1: line 42: the particle growth varies

with particle size, 2) lines 57-58: Oxides of. . ., 3) lines 64-65: Numerous studies. . ., 4)

the paragraph on lines 48-55: there are plenty of fresher papers on this, even reviews,

that could be mentioned here.

Response 4

The following references have been added:

Line 42: *Backman et al., 2012; Gagne et al., 2011; Manninen et al., 2010*

Lines 57-58: *Harrison, 2007; Seinfeld and Pandis, 2006*

Lines 64-65: *; Seinfeld and Pandis, 2006; Suni et al., 2008; Man et al., 2015; Pushpawela et al., 2018*

Lines 48-49: *Kulmala et al., 2004; Backman et al., 2012; Gagne et al., 2011; Manninen et al., 2009, 2010; Rose et al., 2015; Siingh et al., 2013*

Line 53*: Birmili and Wiedensohler, 2000; Kulmala et al., 2004, 2013*

Comment 5

Figure 1a seems unnessary to me, as all the required information can be obtained from

figure 1b. I recommend removing figure 1a from the paper.

Response 5

We have removed Figure 1(a) from the paper.

In response to Reviewer #1, we have replaced this figure with two figures showing the day time and night time NPF events separately as a function of times after sunrise and sunset, respectively.

Response to Anonymous Referee #3

Comment 1

The manuscript presents data from new particle formation (NPF) events in an urban environment in Brisbane, Australia. The main finding is that some NPF events could be misidentified growth of aerosol particles. The main issue is that this interpretation relies solely on the NAIS size distributions measured with the particle mode. The presented size distribution (Fig. 3) has no charger ion signal, which is an indication that the detection of the smallest size fraction was faulty. When the NAIS is adjusted to filter all the corona changer ions, it will also filter the newly formed particles measured within the particle mode. Nevertheless, I would not recommend to plot the corona ions a part of the particle spectra as it is not a real signal from ambient sample.

I would recommend that the authors check the diagnostic values for these days and contact the instrument vendor to determine the quality of the measurements. The comparison of these results to the NAIS ion mode measurements is also extremely important, especially, to understand the performance of their instrument. Authors mention on Page 7, Line 153 that also the ion mode measurements were recorded.

Response 1

We thank the reviewer for pointing this out.

We are aware of the problem with the NAIS and the corona charger ions. We have inserted the following text in the Methods section (Lines 144-149):

"In the particle mode, it uses a corona needle to charge the particles. This leads to an inherent problem where the very small particles cannot be distinguished from the corona ions (Manninen et al., 2016). For this reason, we have restricted the lower detection limit in the particle mode to 2 nm".

As suggested, we have also removed the data below 2 nm from all the particle spectragrams (Figures 2 and 3 have been revised accordingly).

It is probable that the charger ion signal in Figure 3 is 'missing' because of the colour scale used in the diagram. When we adjust the colour scale, the cluster ion band shows up clearly as shown in the figure below:

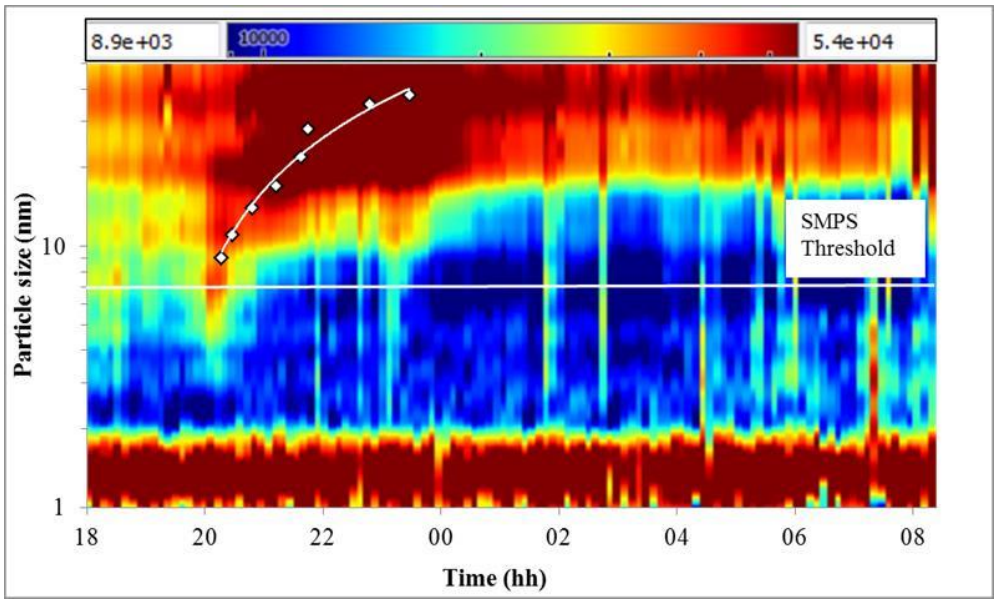

As suggested, we have removed the data below 2 nm and redrawn this figure and it now appears as follows:

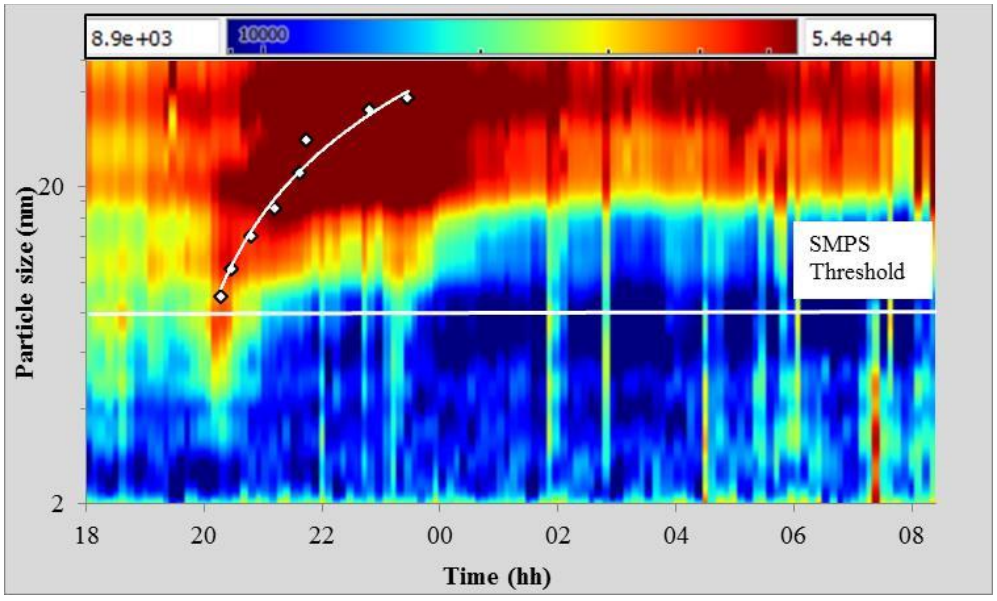

Comment 2

The manuscript also does not reveal the source of the freshly formed 20 nm size particles that grow. It is visible in Figure 5 that the 2 growth only events correlate (at least the 2nd is clearly visible by eye) with an increase in particle number concentration. How well does your SMPS and NAIS agree in particle mode? Show a comparison figure as they overlapping size range.

Please find below a few line by line comments as the missing charger ions are clearly

the largest issue at the moment (see comment to Fig. 3 below):

Response 2

20 nm was the value of the count median diameter of the particles that were present in the atmosphere as measured by the SMPS. These are background particles that arise from a number of sources in the environment, mainly motor vehicle emissions.

Manninen et al (2016) have reported that the NAIS over-estimates the particle number concentration at sizes in the range 20-42 nm. Our results agreed with this observation with a difference of up to a factor of 20% in this size range. This did not create an issue as the particle number concentration in this size range was not quantified nor used in any formulations in this study. We accept that, this will affect the particle number concentrations in the larger sizes in the spectragrams shown in Figures 2 and 3. This was not a big issue as the particle number concentrations are represented in colour contours and were not quantified in these figures. The particle number concentrations in Figures 4, 5 and 6 are not from the NAIS – they are from the SMPS. So, there was no issue there.

Comment 3

L360: Hard to see a growth until the early morning. Was the time series smoothed?

The mean diameter seems to plateau.

Response 3

This refers to Figure 4. There are 4 NPF events in this figure and they are indicated by the red arrows. The particle growth times are shaded in grey. The green line is the median particle diameter and this increases within all four grey shaded boxes. The right edge of each box indicates when the growth ends and these occur during the early hours of the day. If it would make it clearer, we have changed "*early morning*" to "*early hours*".

The SMPS scans were obtained at time intervals of 5 min. The time series were not smoothed.

The mean diameter (green line) does not plateau inside the grey shaded boxes.

Comment 4

L362-365: The description of the what is presented in Fig 5 is a bit limited. Also: what

happened on the 5th June midday.

Response 4

Figure 5 further supports what is presented in Figure 4. It shows two growth events that followed NPF events and an NPF event that was not followed by a growth event.

5th June midday appears to be a particle burst event. A sharp burst of new particles decreases the median particle size to less than 20 nm. The burst lasts for about 2 hours thereby eliminating the possibility of it being due to a motor vehicle emission plume or a person smoking a cigarette etc.

Comment 5

L367-374: Seems out of place in the result part, move this to the discussion or introduction?

Response 5

We do not have a separate discussion part and this paragraph is within the Results and Discussion section. This comparison follows our observations in the previous paragraph. To illustrate this more clearly, we have modified the first sentence as follows, Line 391-392:

"These observations of continued growth of particles following NPF events is a common phenomenon and has been reported by several other researchers".

Comment 6

L367-381: "Time" is the time of day?

Response 6

Yes, it is the Time of Day.

We have replaced the x-axis titles "Time" in Figure 6 (a) and (b) with "Time of day".

Comment 7

L376-381: How does this look for NPF events?

Response 7

Relative humidity increases during the night time. Our observations show an increased growth rate with increasing relative humidity. We did not observe an effect of relative humidity on the frequency of NPF, perhaps because the relative humidity is generally low during the day time. We have reported this in our earlier publications (Jayaratne et al, 2016; Pushpawela et al., 2018).

Comment 8

L398: Factor of 2 not 1.

Response 8

This sentence has now been removed in response to a comment by Reviewer #2.

Comments to Figures:

Fig. 1: To see seasonality or the lack of it, the NPF frequency for each month should

be shown.

Response

The scarcity of data during some months, notably January to March, prevented us from deriving a reliable seasonal distribution chart. Shown below is the chart including all months with at least 10 observational days:

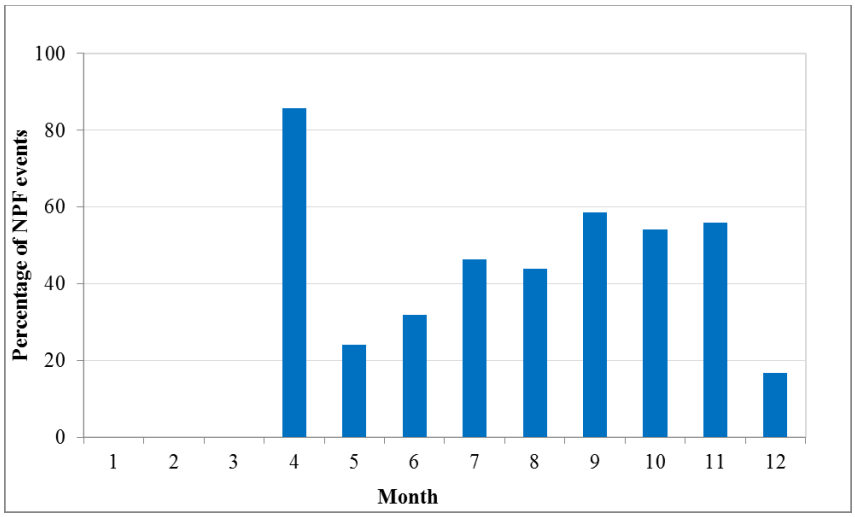

Note that the data spans three calendar years. However, the data for April was from just one year. Hence, the unusually high percentage. The data for December is also from just one year. During this time there were a number of controlled burning events around Brisbane and this accounted for the low percentage of NPF events. The seasonal dependence chart, in our opinion, is not reliable enough to be presented in this paper.

Fig. 2: Data below 2 nm is from charger ions, so it's not a signal but an artifact.

Response

The graphs have been revised and now show only the values above 2 nm (See response to Comment 1 above).

Fig. 3: Why are there almost no charger ions (the signal below about 2nm) in this

figure? This could indicate a problem with the detection of small aerosol particles in

the NAIS. Compare charger ions in Figure 3 to those in Figure 2.

Response

See response to Comment 1 above.

Fig. 4 & 5: Was the time series smoothed? It looks rather noisy.

Response

As stated in Response 3, the SMPS scans were obtained at time intervals of 5 min. The time series were not smoothed. The noise is normal in an urban environment where the dominant source of aerosols, particularly ultrafine particles, are from motor vehicles.

Fig. 6 & 7: The effect shown in Fig 7 is not visible in Fig 6. Plotting diameter vs RH in Figure 6 would allow immediate comparison with Fig 7.

Response

In response to Reviewer#2 (Comment 3), we have removed Figure 7 from the paper. As such, there is no need for a comparison with Fig 6.

Differentiating between particle formation and growth events in an urban environment

Buddhi Pushpawela, Rohan Jayaratne, and Lidia Morawska*

International Laboratory for Air Quality and Health

Queensland University of Technology

GPO Box 2434, Brisbane, QLD 4001, Australia

~~To be~~Revised and submitted to

Atmospheric Chemistry and Physics

~~February~~ June 2018

* Corresponding author contact details:

Tel: (617) 3138 2616; Fax: (617) 3138 9079

Email: l.morawska@qut.edu.au

Abstract

Small aerosols at a given location in the atmosphere often originate in-situ from new particle formation (NPF). However, they can also be produced and then transported from a distant location to the point of observation where they may continue to grow to larger sizes. This study was carried out in the subtropical urban environment of Brisbane, Australia, in order to assess the relative occurrence frequencies of NPF events and particle growth events with no NPF. We used a neutral cluster and air ion spectrometer (NAIS) to monitor particles and ions in the size range 2-42 nm on 485 days, and identified 236 NPF events on 213 days. The majority of these events (37%) occurred during the daylight hours with just 10% at night. However, the NAIS also showed particle growth with no NPF on many nights (28%). Using a scanning mobility particle sizer (SMPS), we showed that particle growth continued at larger sizes and occurred on 70% of nights, typically under high relative humidities. Most particles in the air, especially near coastal locations, contain hygroscopic salts such as sodium chloride that may exhibit deliquescence when the relative humidity exceeds about 75%. The growth rates of particles at night often exceeded the rates observed during NPF events. Although most of these night time growth events were preceded by daytime NPF events, the latter was not a prerequisite for growth. We conclude that particle growth in the atmosphere can be easily misidentified as NPF, especially when they are monitored by an instrument that cannot detect them at the very small sizes.

Keywords: New particle formation, particle growth, atmospheric aerosols, secondary particles.

1 Introduction

The formation of secondary particles in the atmosphere through homogeneous nucleation is known as new particle formation (NPF). This is one of the major sources of particles in the atmosphere. The condensable species that contribute are mainly sulfuric acid and semivolatile organic compounds and the process is thought to occur by binary water-sulfuric-acid or ternary water-sulfuric-acid-ammonia nucleation. Particles, thus formed, form stable clusters that continue to grow to larger sized particles by vapour condensation or by coagulation with other particles (Kulmala et al., 2013).

The particle formation rate and the particle growth rate are the two most important parameters used to characterize an NPF event. The particle formation rate is the rate of formation of smallest measurable size of the particles, generally in the size range 2-3 nm. This is different to the actual nucleation rate (the rate at which the stable clusters form). The particle growth rate varies with particle size (Manninen et al., 2010;Gagné et al., 2011;Backman et al., 2012) and, hence, the reported values depend on the detectable size ranges of the instruments used. Until recently, studies have been limited to measure the particles above 3 nm. However, it is only during the past decade that the advancement of instruments has developed to such a level that particles of 2 nm or even smaller can be measured (Kulmala et al., 2012).

NPF has been observed under a range of environmental conditions, on every continent in the world (Kulmala et al., 2004;Backman et al., 2012;Gagné et al., 2011;Manninen et al., 2009;Manninen et al., 2010;Rose et al., 2015;Pushpawela et al., 2018;Jayaratne et al., 2017). The occurrence rate of NPF is mainly dependent on the nature and concentration of gaseous

precursors, which are controlled by a number of factors including the type and intensity of the sources, concentration of pre-existing aerosols, origin of air masses, photo-chemical processes and meteorological parameters such as intensity of solar radiation, temperature, relative humidity, wind direction and wind speed (Birmili and Wiedensohler, 2000;Kulmala et al., 2004;Kulmala et al., 2013). Pre-existing aerosols act as sinks to condensable gases that are present in the atmosphere. This leads to a reduction in their vapour pressure and inhibits homogeneous nucleation.

Oxides of nitrogen and volatile organic compounds are readily produced in urban environments from sources such as motor vehicles and industrial facilities (Seinfeld and Pandis, 2006;Harrison, 2007). These gases react with ozone in the presence of sunlight to produce OH radicals that can oxidise gaseous precursors such as sulphur dioxide and nitric oxide, converting them into the condensable species sulfuric acid and nitric acid, respectively. These photochemical reactions are more likely to occur during the day time on sunny days with high intensity of solar radiation, which is when we would expect to observe more NPF events.

Numerous studies in many different environments have conclusively shown that the large majority of NPF occur during the day time (Seinfeld and Pandis, 2006;Suni et al., 2008;Man et al., 2015;Pushpawela et al., 2018). Very few studies have reported the occurrence of NPF during the night time and these have mostly been in forest environments and coastal sites. Table 1 gives a summary of studies in chronological order, that have reported observations and frequencies of occurrence of night time NPF events, together with the respective frequencies of occurrence of day time NPF events and the instrumentation that was used. We

see that, at a given location, NPF events were generally more likely to occur during the day time than during the night. The sole exception is the short study of 16 days by Kammer et al. (2017). Night time events were reported on between 4% and 37% of the days observed. They were more likely to be observed at forest locations (16% to 37%), while the two studies conducted at coastal locations showed significantly lower values of 4% and 11%. In a previous study carried out in and around Brisbane with an SMPS, Salimi et al. (2017) reported NPF events on around one in every four nights. They also reported NPF on every second day which is significantly higher than any of the values found in Brisbane (Guo et al., 2008;Cheung et al., 2011;Crilley et al., 2014;Jayaratne et al., 2016;Pushpawela et al., 2018).

In the present study, we collected data of charged and uncharged particle concentrations in the urban environment of Brisbane using a neutral cluster and air ion spectrometer (NAIS) on close to five hundred days. The NAIS can provide more accurate information on NPF than the SMPS, because of its ability to measure particles down to 2 nm in size, which is very close to the size at which the initial steps of nucleation and formation of particles occur (Manninen et al., 2011;Manninen et al., 2016). The results were compared with that obtained simultaneously with an SMPS with a minimum detectable size of 9 nm. The SMPS data were also used to determine the growth rates of particles. The observations by the NAIS and SMPS were used to differentiate between (a) local NPF events followed by particle growth and (b) growth events in the absence of NPF events – two phenomena that are not always concurrent and often misidentified when only one instrument is used.

2 Methods

2.1 Monitoring Site

The instruments were housed in a sixth-floor laboratory in a building at the Gardens Point campus of the Queensland University of Technology in Brisbane, Australia. The site is situated at the edge of the Brisbane Central Business District bordered by the City Botanical Gardens and the Brisbane River, approximately 100 m away from a busy motorway carrying about 120,000 vehicles per day and is representative of a typical urban environment in Australia. The measurements were carried out during the three calendar years 2012, 2015 and 2017, yielding 485 complete days of data.

The pollutants at this site were mainly from motor vehicle exhaust emissions. Depending on the wind direction, emissions may also be received from the Port of Brisbane and two oil refineries in its vicinity as well as from Brisbane Airport, all located about 20 km to the north-east of the monitoring site.

Meteorological data such as temperature, relative humidity, solar radiation, rainfall, wind direction and wind speed as well as air quality data such as sulphur dioxide (SO_2), ozone (O_3), PM_{10}, $PM_{2.5}$ and atmospheric visibility were obtained from the Department of Environmental and Heritage Protection, Queensland, at their in-situ site at the Queensland University of Technology and two other sites within a distance of 1.5 km from the University.

2.2 Description of the instruments

The NAIS, manufactured by Airel Ltd, Estonia (Manninen et al., 2016), detects the mobility distribution of charged clusters and particles of both polarities in the electrical mobility range from 3.2 to 0.0013 $cm^2\ V^{-1}s^{-1}$. It also measures the size distribution of total particles in the size range from 2.0 - 42 nm. The instrument has a high-resolution time down to 1 s and consists of two cylindrical electrical mobility analysers, one for each polarity. It operates in

four modes: ion mode; particle mode; alternate charging mode and offset mode. In the ion mode, the NAIS measures naturally charged particles without any modification. In the particle mode, it uses a corona needle to charge the particles. This leads to an inherent problem where the very small particles cannot be distinguished from the corona ions (Manninen et al., 2016). ~~measures all charged and uncharged particles. The~~ For this reason, we have restricted the lower detection limit in the particle mode ~~is restricted~~ to 2 nm ~~due to presence of corona generated ions in the instrument (Manninen et al., 2016)~~. The alternate charging mode is similar to the particle mode, but it electrically neutralizes the sampled particles and improves the performance of the instrument. In the offset mode, the NAIS measures zero signals, noise levels and parasitic currents. The measurement process of the instrument is fully automated. The measurement cycle of the NAIS varies from 2-5 minutes. A more detailed discussion of its design and principles is given in (Manninen et al., 2011) and (Mirme and Mirme, 2013). In this study, we set the measurement cycle to 2 min ion mode, 2 min particle mode, and 1 min offset mode.

An SMPS, consisting of a TSI model 3071 differential mobility analyser and a TSI model 3782 condensation particle counter, was used to measure the particle size distribution in the range from 9 - 415 nm.

2.3 Data Analysis

2.3.1 Classification of New Particle Formation (NPF) events:

We identified NPF events using the rate of change of total particle concentration, dN/dt, where N is the number of particles in the size range 2.0 -10.0 nm and using the classification described by (Zhang et al., 2004). Events with N > 10,000 cm^{-3} for at least 1 hour and dN/dt >10,000 $cm^{-3}h^{-1}$ were defined as "strong" NPF events. Events with 5000 < N < 10,000 cm^{-3}

for at least 1 hour and 5000 < dN/dt < 10,000 $cm^{-3}h^{-1}$ were classified as "weak" NPF events. All of these events started in the nucleation mode size range and prevailed over a time span of more than one hour, generally exhibiting a "banana" shape in the time-series contour plot of particle number concentration (PNC), indicating particle formation and subsequent growth. A 24-hour day that included at least one NPF event was labelled as an 'NPF Day'. A day on which there were no NPF events was labelled as a 'Non-event Day'.

Every NPF event was characterised by a sharp increase of the PNC in the intermediate size range from 2.0-7.0 nm. This observation has been used to determine the starting time of an NPF event (Leino et al., 2016). Similarly, in the present study, the starting time of a strong NPF event was determined by noting the time of first occurrence of dN/dt > 10,000 $cm^{-3}h^{-1}$. The starting time of a weak NPF event was determined by noting the time of first occurrence of dN/dt > 5000 $cm^{-3}h^{-1}$. N is the number of particles in the size range 2.0-10 nm.

NPF events that started between ~~6:00 am~~sunrise and ~~6:00 pm~~sunset were categorized as "day time" NPF. NPF events that started between ~~6:00 pm~~sunset and ~~6:00 am~~sunrise were categorized as "night time" NPF.

2.3.2 Classification of Growth events:

The data from the NAIS showed that growth events were not always preceded by an NPF event. Growth events that did not follow an NPF appeared as a "floating-banana" shape in the PNC contour plots. These events were identified using the rate of change in the diameter (d_p) of particle, dd_P/dt. Events with dd_p/dt > 1 nm h^{-1} were classified as "growth" events. In the NAIS data, these events showed an enhancement of PNC in the size range above 7 nm. Further, in these events, unlike in NPF events, the sharp increase in PNC in the size range between 2-7 nm was absent. In this way, growth events could be clearly distinguished from

NPF events. In fact, unless they were preceded by an NPF event, most growth events showed very few particles in the size range below 10 nm. We also observed "vertical band" shapes which were due to the sudden appearance of high concentrations of particles in all sizes. These were neither NPF nor growth events and characterised the influx of already formed particles from further locations to the monitoring site, and were ignored in the analysis.

2.3.3 Calculation of particles growth rate

The growth rate (GR) of particles is defined as

$$\boldsymbol{GR} = \frac{\boldsymbol{dd_p}}{\boldsymbol{dt}} = \frac{\boldsymbol{d_{p2} - d_{p1}}}{\boldsymbol{t_2 - t_1}} \quad (1)$$

where dp_2 and dp_1 are the diameters of particles at times t_1 and t_2. This was calculated by the maximum concentration method described in (Kulmala et al., 2012). The unit of the GR is nanometres per hour. During an NPF or a growth event, the number concentration of small particles increases, showing a peak in the particle size distribution. When the particles grow in size, this peak shifts towards larger sizes. In order to derive the maximum particle concentration, we plotted the time series of the PNC in different size ranges. We estimated the GR from the slope of the best-fitted line on the graph of mid-point diameter of particles versus the time of maximum concentration (Dos Santos et al., 2015;Pierce et al., 2014).

2.3.4 Statistically significant differences

Statistical significances of the difference between two parameters were calculated using the Student's t test.

3. Results and Discussion

3.1 Observation of NPF during study period

The study yielded complete 24h data on a total of 485 days. The instrument was unavailable on some days, as it was required for other projects or was being serviced or cleaned. In addition, a few days were 'lost' due to missing data owing to power failures or instrument malfunction. A summary of the observational periods, together with the corresponding number of days on which 24h data were available and NPF events were observed, is shown in Table 2. Columns 3 to 8 represent the number of day time, night time and total NPF classified into strong and weak events according to the method described in section 2.3.1. The last three columns give a summary of all NPF events.

Altogether, 236 NPF events (strong and weak) were observed on 213 of the 485 days on which we were able to obtain data. Out of this, strong NPF events were observed on 177 days, giving an occurrence rate of 37%. This is only slightly less than the rate of 41% found by Pushpawela et al. (2018) using the NAIS in Brisbane over the single calendar year 2012. In the two other studies using the NAIS in Brisbane, Crilley et al. (2014) and Jayaratne et al. (2016) reported higher values of 56% and 45% respectively. However, both these previous studies used a slightly different criteria to identify NPF events, that is they excluded the requirement of $N > 10{,}000$ cm^{-3} for a period of at least 1 hour. The Crilley et al. (2014) study was also conducted over a much shorter period of 36 days only. Table 2 also shows that, although "strong" day time NPF events were observed on 159 days (33%), "strong" night time NPFs were relatively scarce, occurring on just 18 days (4%). Further, "weak" NPF events were observed on 59 days (12%) and these were almost equally distributed between

night and day times. Taking into account all strong and weak NPF, day time NPF occurred on 37% of the days while night time NPF occurred on only 10%. In Table 2, it should be noted that a given day may sometimes have both a day time and a night time event. There were 23 such days. In addition, there were 8 days that had two daytime events and no instances of two events during the same night. There have been three previous studies that have used an SMPS to study NPF in Brisbane. Together with the occurrence rates in parenthesis, these were Guo et al. (2008) (35%), Cheung et al. (2011) (26%) and Salimi et al. (2017) (77%).

3.2 Diurnal variation

Figures 1 (a) and (b) shows ~~a~~the summary of starting times of all NPF events during the day time and night time, respectively, estimated by using the method described in Section 2.3.1. ~~Figure 1 (b) shows t~~The histograms ~~of~~ show the number of events observed in each 30 min period ~~of the day~~after sunrise and sunset, respectively. The times indicated on the x-axis refer to the end of each 30 min period. In Figure 1(a), the three bars at the extreme left correspond to times before sunrise. We have classified these as night time events. Both of these figures show that most NPF events (~~73~~71%) began during the morning, with a high likelihood of occurrence between 2 and 4 hours after sunrise, corresponding to approximately between 8.00 am and 10.00 am. In particular, ~~85out~~ 90 out of 236 events occurred during this 2-hour period. This is likely to be a result of several factors such as the higher concentration of precursor gases from motor vehicles during the morning rush hour and the onset of solar radiation. However, no NPF were observed during the evening rush hour period around 4-6 pm. During this time, the air temperatures are still relatively high and, although the gaseous precursors are being produced, the vapour pressures may not be sufficiently high to produce

secondary particles. The starting times of night time NPF events also showed a distinct trend with a peak likelihood between 3 and 4 hours after sunset, corresponding to approximately 8 and 9 pm. By this time of the day, the temperatures have generally fallen sufficiently for vapour pressures to increase. No night time events were observed at all during the second half of the night, between 11 pm and 4 am. Although the temperatures are low during this time, there is minimum production of precursor gases.

3.3 Effect of atmospheric parameters

A summary of the mean and range of various meteorological and air quality parameters during NPF and non-event days is shown in Table 3. The mean solar radiation intensity on NPF days were significantly higher compared to the other days with mean values of 505 W m^{-2} and 397 W m^{-2}, respectively. Conversely, the mean relative humidity on NPF days was significantly less than on other days with values of 54% and 66%, respectively. The mean relative humidity on NPF days were 59% and 52% during winter and summer months. Therefore, NPF events were more likely to occur on days with low relative humidity and high solar radiation. Similar observations have been reported from several other urban cites such as Melpitz, Germany (Birmili and Wiedensohler, 2000), San Pietro Capofiume, Italy (Hamed et al., 2007) and Pune, India (Kanawade et al., 2014).

The wind direction on NPF days was mainly from the south to southwest directions, with a mean wind speed of around 1.4 m s^{-1}. The mean air temperature was 17^0C and 24^0C on NPF days during winter and summer months. We did not detect any clear differences in wind direction, wind speed and air temperature between NPF days and the other days. In general, most of the NPF events occurred on days when there was no rainfall observed. However, a

clear dependence was found between NPF occurrence and atmospheric visibility. The visibility was expressed through the particle back scatter coefficient (BSP) in units of Mm^{-1}. These two parameters are inversely proportional to each other. The BSP observed at 8 am on NPF days was significantly lower on NPF days than on other days, with mean values of 18 $Mm^{-1}$and 31 Mm^{-1}, respectively. A good discussion about the relationship between the occurrence of NPF in Brisbane and the values of BSP may be found in Jayaratne et al. (2015). This study also found that, no NPF events occurred on days when the mean $PM_{2.5}$ exceeded 20 $\mu g\ m^{-3}$ in Brisbane.

The presence of high concentration of O_3 under high solar radiation increases the production of OH radicals, and the presence of high concentration of both SO_2 and OH radicals give rise to increased production of H_2SO_4 leading to NPF (Seinfeld and Pandis, 2006;Lee et al., 2008). Therefore, we would expect SO_2 and O_3 concentration levels to be higher on NPF days than on non-event days. However, we observed only a marginal increase of SO_2 and O_3 concentrations on NPF days (Table 3).

3.4 Day time and night time NPF events

The two upper panels in Figure 2 show the NAIS spectragrams obtained between 8:00 am and 4:00 pm on 19 August 2017 and 31 July 2015, respectively. On 19 August, a strong NPF event began in the morning at around 9:00 am and lasted for 4-5 hours. Here, the total PNC increased from about 30,000 cm^{-3} at 9:00 am to just over 90,000 cm^{-3} at 11:00 am, giving a particle formation rate of 30,000 $cm^{-3}\ h^{-1}$. Thereafter, particles continued to grow in size for several hours. The PNC decreased gradually in the afternoon. The particles showed a relatively high growth rate of about 7 nm h^{-1} in the size range 2-42 nm.

The two lower panels in Figure 2 show NAIS spectragrams obtained during the night, between 6:00 pm and 2:00 am on 20 August 2015 and 5 September 2015, respectively. On 20 August, a strong NPF event began in the night at around 9:30 pm and lasted for 2-3 hours. The particles also showed a relatively high growth rate of about 11 nm h^{-1} in the size range 2-42 nm.

We did not observe a significant difference in growth rates of particles between daytime and night time NPF events. ~~Typically, the growth rates were high during the first few hours and then decreased to a few nanometres per hour within 3-4 hours after nucleation.~~ The growth rate of particles in the size range 2-42 nm during all NPF events, calculated from equation (1), varied between 4 nm h^{-1} and 22 nm h^{-1} with a mean and standard deviation of (12.1 ± 6.5) nm h^{-1}.

These growth rates were comparable to the values reported at two other urban locations; Atlanta, USA (3-20 nm h^{-1})(Stolzenburg et al., 2005) and Budapest, Hungary (2-13 nm h^{-1}) (Salma et al., 2011). However, the mean values of growth rates obtained by previous studies in Brisbane were significantly lower than the value reported by this study. For example, Cheung et al. (2011) and Salimi et al. (2017) reported growth rates of 4.6 nm h^{-1} and 2.4 nm h^{-1} respectively. Both these studies were carried out using an SMPS with a lower detection size of about 10 nm.

Typically, the particle growth rates were high during the first few hours and then decreased to a few nanometres per hour within 3-4 hours after nucleation. Several studies have reported that the growth rate of particles in the size range 7-20 nm was greater than that in the smaller size range 3-7 nm (Manninen et al., 2010;Gagné et al., 2011;Yli-Juuti et al., 2009;Backman et al., 2012). Manninen et al. (2010) studied NPF events at 12 European sites and found that 9

out of the 12 sites showed this trend while at 3 sites the growth rate was greater in the smaller size range. They suggested that this size dependence was due to different condensing vapours participating in the growth of different sized particles depending on their saturation vapour pressures. For example, it is well known that sulfuric acid plays a dominant role in nucleation and the initial growth of particles during NPF while organics dominate the growth at larger sizes of 10-30 nm (Yli-Juuti et al., 2011;Manninen et al., 2009;Smith et al., 2008). Further evidence comes from the observation that the growth rate of the particles in the larger size range of 7-20 nm is enhanced during the summer when the concentration of biogenic volatile organic compounds in the atmosphere is greater (Yli-Juuti et al., 2011). Our observations of particle growth rates in the different size ranges agree with previous studies that have suggested that the dominant condensable vapour in Brisbane is probably sulfuric acid, with organics playing a secondary role (Crilley et al., 2014).

3.5 Observations of growth events during the study period

NPF events are almost always followed by particle growth. However, with the NAIS, we observed several growth events that were not preceded by an NPF event. These events were observed more often at night than during the day. A summary of these events observed by the NAIS, is shown in Table 4. Columns 3 to 5 represent the number of day time, night time and total growth events classified according to the method described in section 2.3.2. Figure 3 shows examples of NAIS spectragrams of such growth events that occurred during the day time (a) and night time (b). Particle growth is again demonstrated by the typical banana shape of the colour contours, with the difference that the lower end of the 'banana' does not reach as far as the smallest particle sizes, indicating that there is no NPF. This shape is sometimes referred to as a "floating banana", to differentiate it from the complete "banana" shape of an

NPF event. In most of the events, particle growth is observed to continue for several hours. The observed rates of growth varied between 1 nm h^{-1} and 45 nm h^{-1} with a mean and standard deviation of (16.8 ± 11.9) nm h^{-1} in the size range 8-42 nm. During the 485 days of observation, excluding NPF events, day time growth events were observed on just 54 days (11%), whereas night time growth events were observed on 135 days (28%). The overall occurrence rate of growth events obtained by the NAIS was 37%. However, it should be noted that particles continued to grow at sizes larger than the upper size detection rate of the NAIS, which was 42 nm. Thus, the SMPS was likely to detect many more growth events than the NAIS.

3.6 Observations of particle growth by SMPS

Next, we look at the behaviour of total PNC and the median particle diameter of NPF and growth events using the data obtained by the SMPS. Figure 4 shows a period of 6 days, during which there were 3 consecutive daytime NPF events that were followed by two non-event days and a day with a daytime NPF event. The NPF events are shown by red arrows. In each of these four cases, prior to the inception of the daytime NPF, the total PNC was low - about 2500 cm^{-3}. During the NPF event, the total PNC increased from about 5000 cm^{-3} in the morning to over 15,000 cm^{-3} near mid-day. Thereafter, the particles started to grow in size up to 20-30 nm. During and after the late afternoon, although the total PNC began to decrease, the particles continued to grow in size up to 40-65 nm. All 4 NPF events continued through this "second phase of particle growth" until the early ~~morning~~ hours of the next day. The growth rate varied between 2-7 nm h^{-1}.

Figure 5 shows another example. During this 7 day period, two growth events in the late afternoon were preceded by NPF events. The remaining two growth events did not follow

any NPF event. The particles grew up to 40-50 nm. During the measurement period, particle growth events were observed on 65-70% of the nights.

These observations of ~~C~~continued growth of particles following NPF events is a common phenomenon and has~~ve~~ been reported by several other researchers. For example, Man et al. (2015) observed 12 out of 17 NPF events with particle growth from 10 nm to 40 nm during the day time at a suburban coastal site in Hong Kong. In addition, they observed 3 events with second phase of particle growth to 61-97 nm at night time. These three events were preceded by a daytime NPF event. Russell et al. (2007) observed nanoparticle growth on 19 out of 48 days (40%) during the day time and on 5 out of 48 days (10%) during the night time in Appledore Island, Maine, USA. Subsequently, particle growth continued over several hours with rates varying from 3 to 13 nm h^{-1}.

NPF generally occur at high solar radiation, high temperature and low relative humidity. However, growth events were more likely to occur during time periods with low temperature and high relative humidity. We investigated this further by plotting the median particle size and relative humidity as a function of time during growth events (Figure 6). In general, progression into the night time, after 6:00 pm, was accompanied by a decrease in air temperature, resulting in an increase in relative humidity in the atmosphere.

During the event that occurred on July 16, 2012 the median particle size increased from about 30 to 65 nm as the relative humidity increased from 65% to 80% (Figure 6a). Similarly, during the event that occurred on July 20, 2012 the median particle size increased from about 30 to 75 nm as the relative humidity increased from 75% to 90% (Figure 6b).

It is well-known that relative humidity may favour particle growth in the atmosphere owing to several reasons. For example, atmospheric aerosol particles ~~change their~~increase in size with relative humidity due to the uptake of water (Winkler, 1988). In addition, when the relative humidity increases, heterogeneous reactions can take place in the liquid phase of a growing particle while, if there is an accompanying drop in temperature, it would enhance the transport of semivolatile compounds from the gas phase on to the surface of the particles. Water uptake is caused by the deliquescence of soluble salts which form a solution when the solid compound is exposed to water vapour at sufficiently high vapour pressure. Several organic materials are also known to absorb water at high humidity which is more generally known as hygroscopicity. ~~Figure 7 shows the diameter of a s~~Sodium chloride (NaCl) ~~-bearing particle as a function of relative humidity (Wise et al., 2007). The red line corresponds to the~~has a deliquescence point ~~for NaCl at~~of 76% relative humidity. At this point, ~~the~~ a NaCl-bearing particle will deliquesce~~s~~ and become~~s~~ a solution of droplet with a well-defined spherical shape. The particle diameter does not change considerably as the relative humidity is increased from 0 to 74%, beyond which it can increase considerably. ~~As the relative humidity increased from 76% to 91%, the particle diameter increased by a factor of 1 or more. Therefore, as the relative humidity increases, the particles sizes increase due to their affinity to absorb water.~~ Close to the coast, sea-salt aerosols constitute a large proportion of the atmospheric particulate mass and NaCl is a major component. Many of the inorganic substances that readily absorb water, such as sea salt, ammonium salts and nitrates, are present in the Brisbane environment (Harrison, 2007). Therefore, it is not surprising that, in the present study, we observed that particle growth occurred on 7 out of 10 nights with high relative humidity.

3.7 Probability of growth events being misidentified as NPF events

In Figure 3 (a), the horizontal white line indicates the typical lower size detection threshold of the SMPS that has been used in many locations before; we chose 7 nm as a typical value in this case. The SMPS does not 'see' any particles below this line. It is clear that there is an enhancement of PNC in the size range 7-20 nm around 11:30 am on this day. The absence of intermediate size particles (between 2-7 nm) suggests that the 7-20 nm particles originated on-site by primary emission or were advected to the site from a distant location. The NAIS clearly shows that this was not an NPF event. However, in the absence of information below a particle size of 7 nm, the SMPS data may be easily misinterpreted as an NPF event. The typical 'floating banana' shape of the spectragram contours show that the particles continue to grow between 11:30 a.m. and about 1:00 p.m. and this can be observed by an SMPS. As we have demonstrated, growth events are not always formation events. There are two enhancement events near 1.00 pm and 3.30 pm. Once again, the NAIS shows that neither of these are NPF events, although based on the SMPS they may be mistakenly identified as such. Figure 3 (b) shows another event that can be easily misidentified as an NPF event based on SMPS data alone.

Salimi et al. (2017), using an SMPS with a lower size limit of 9 nm at 25 sites across Brisbane, reported 219 NPF events out of 285 days of measurements. This occurrence rate of 77% (67% of day time and 33% of night time) is significantly higher than any of the values found previously in Brisbane and at any other location in the world. With the NAIS, it was possible to show that most of these events were growth events and not NPF events. It was not possible to differentiate these two types of events with the SMPS alone as it provides no knowledge of the PNC below 9 nm. With the NAIS, we did not observe nocturnal NPF events on more than 47 of 500 days.

In many NPF events, particle growth ceases after they have grown to a certain size. In the growth event in Figure 3, the maximum size is about 25 nm. In such cases, the greater part of the 'banana' profile is below 7 nm and, thus, invisible to the SMPS. This could result in the missing of such NPF events. Considering, all the factors above, it is clear that the NAIS has a distinct advantage over the SMPS in correctly identifying NPF events in the atmosphere.

4. Summary and Conclusions

We monitored charged and neutral PNCs in the size range 2-42 nm on nearly 500 days over three calendar years in the urban environment of Brisbane, Australia, using a NAIS. The data were used to differentiate between NPF events and growth events with no NPF. Day time NPF events were observed on 37% of the observational days, with night time events on only 10% of the days. NPF events were more likely to occur on days with low relative humidity and high solar radiation. 7~~3~~1% of NPF events occurred during the morning, with the highest probability of occurrence between 2 and 4 hours after sunrise, corresponding to approximately between 8.00 am and 10.00 am. Most of the night time events occurred between 3 and 4 hours after sunset, corresponding to approximately between 8.00 pm and 9:00 pm. No night time events were observed between 11.00 pm and 4.00 am. 28% of the particle growth events that occurred at night were not preceded by an NPF event. These events were characterized by high growth rates of up to 45 nm h^{-1}. The SMPS results showed that particle growth continued at larger sizes from ~40 nm to 70 nm and occurred on 70% of nights. Maximum relative humidities were over 80% on most of these nights. These results show that, when particles are monitored by an instrument such as the SMPS that cannot detect them at the very small sizes, particle growth in the atmosphere may be easily misidentified as NPF, leading to an overestimation of the frequency of the latter.

Acknowledgements

We are thankful to the Department of Environmental and Heritage Protection, Queensland, for providing some of the meteorological data used in this study.

References:

Backman, J., Rizzo, L. V., Hakala, J., Nieminen, T., Manninen, H. E., Morais, F., Aalto, P. P., Siivola, E., Carbone, S., and Hillamo, R.: On the diurnal cycle of urban aerosols, black carbon and the occurrence of new particle formation events in springtime São Paulo, Brazil, Atmospheric Chemistry and Physics, 12, 11733-11751, 2012.

Birmili, W., and Wiedensohler, A.: New particle formation in the continental boundary layer: Meteorological and gas phase parameter influence, Geophysical Research Letters, 27, 3325-3328, 2000.

Cheung, H., Morawska, L., and Ristovski, Z.: Observation of new particle formation in subtropical urban environment, Atmospheric Chemistry and Physics, 11, 3823, 2011.

Crilley, L. R., Jayaratne, E. R., Ayoko, G. A., Miljevic, B., Ristovski, Z., and Morawska, L.: Observations on the formation, growth and chemical composition of aerosols in an urban environment, Environmental science & technology, 48, 6588-6596, 2014.

Dos Santos, V., Herrmann, E., Manninen, H., Hussein, T., Hakala, J., Nieminen, T., Aalto, P., Merkel, M., Wiedensohler, A., and Kulmala, M.: Variability of air ion concentrations in urban Paris, Atmospheric Chemistry and Physics, 15, 13717-13737, 2015.

Gagné, S., Lehtipalo, K., Manninen, H., Nieminen, T., Schobesberger, S., Franchin, A., Yli-Juuti, T., Boulon, J., Sonntag, A., and Mirme, S.: Intercomparison of air ion spectrometers: an evaluation of results in varying conditions, Atmospheric Measurement Techniques, 4, 805-822, 2011.

Guo, H., Ding, A., Morawska, L., He, C., Ayoko, G., Li, Y. S., and Hung, W. T.: Size distribution and new particle formation in subtropical eastern Australia, Environ. Chem., 5, 382-390, 2008.

514 Hamed, A., Joutsensaari, J., Mikkonen, S., Sogacheva, L., Maso, M. D., Kulmala, M.,
515 Cavalli, F., Fuzzi, S., Facchini, M., and Decesari, S.: Nucleation and growth of new particles
516 in Po Valley, Italy, Atmospheric Chemistry and Physics, 7, 355-376, 2007.
517 Harrison, R. M.: Understanding our environment: an introduction to environmental chemistry
518 and pollution, Royal Society of chemistry, 2007.
519 Jayaratne, E. R., Clifford, S., and Morawska, L.: Atmospheric Visibility and PM10 as
520 Indicators of New Particle Formation in an Urban Environment, Environmental Science &
521 Technology, 49, 12751-12757, 10.1021/acs.est.5b01851, 2015.
522 Jayaratne, E. R., Pushpawela, B., and Morawska, L.: Temporal evolution of charged and
523 neutral nanoparticle concentrations during atmospheric new particle formation events and its
524 implications for ion-induced nucleation, Frontiers of Environmental Science & Engineering,
525 10, 13, 2016.
526 Jayaratne, R., Pushpawela, B., He, C., Li, H., Gao, J., Chai, F., and Morawska, L.:
527 Observations of particles at their formation sizes in Beijing, China, Atmos. Chem. Phys., 17,
528 8825-8835, 10.5194/acp-17-8825-2017, 2017.
529 Junninen, H., Hulkkonen, M., Riipinen, I., Nieminen, T., Hirsikko, A., Suni, T., Boy, M.,
530 LEE, S. H., Vana, M., and Tammet, H.: Observations on nocturnal growth of atmospheric
531 clusters, Tellus B, 60, 365-371, 2008.
532 Kalivitis, N., Stavroulas, I., Bougiatioti, A., Kouvarakis, G., Gagné, S., Manninen, H.,
533 Kulmala, M., and Mihalopoulos, N.: Night-time enhanced atmospheric ion concentrations in
534 the marine boundary layer, Atmospheric Chemistry and Physics, 12, 3627-3638, 2012.
535 Kammer, J., Perraudin, E., Flaud, P.-M., Lamaud, E., Bonnefond, J., and Villenave, E.:
536 Observation of nighttime new particle formation over the French Landes forest, Science of
537 The Total Environment, 2017.

538 Kanawade, V., Tripathi, S. N., Siingh, D., Gautam, A. S., Srivastava, A. K., Kamra, A. K.,
539 Soni, V. K., and Sethi, V.: Observations of new particle formation at two distinct Indian
540 subcontinental urban locations, Atmos. Environ., 96, 370-379, 2014.
541 Kulmala, M., Vehkamäki, H., Petäjä, T., Dal Maso, M., Lauri, A., Kerminen, V.-M., Birmili,
542 W., and McMurry, P. H.: Formation and growth rates of ultrafine atmospheric particles: a
543 review of observations, J. Aerosol Sci., 35, 143-176, 2004.
544 Kulmala, M., Petäjä, T., Nieminen, T., Sipilä, M., Manninen, H. E., Lehtipalo, K., Dal Maso,
545 M., Aalto, P. P., Junninen, H., and Paasonen, P.: Measurement of the nucleation of
546 atmospheric aerosol particles, Nature protocols, 7, 1651-1667, 2012.
547 Kulmala, M., Kontkanen, J., Junninen, H., Lehtipalo, K., Manninen, H. E., Nieminen, T.,
548 Petäjä, T., Sipilä, M., Schobesberger, S., and Rantala, P.: Direct observations of atmospheric
549 aerosol nucleation, Science, 339, 943-946, 2013.
550 Lee, S. H., Young, L. H., Benson, D. R., Suni, T., Kulmala, M., Junninen, H., Campos, T. L.,
551 Rogers, D. C., and Jensen, J.: Observations of nighttime new particle formation in the
552 troposphere, Journal of Geophysical Research: Atmospheres (1984–2012), 113, 2008.
553 Leino, K., Nieminen, T., Manninen, H. E., Petäjä, T., Kerminen, V.-M., and Kulmala, M.:
554 Intermediate ions as a strong indicator of new particle formation bursts in a boreal forest,
555 Boreal Environment Research, 2016.
556 Man, H., Zhu, Y., Ji, F., Yao, X., Lau, N. T., Li, Y., Lee, B. P., and Chan, C. K.: Comparison
557 of daytime and nighttime new particle growth at the HKUST supersite in Hong Kong,
558 Environmental science & technology, 49, 7170-7178, 2015.
559 Manninen, H., Nieminen, T., Riipinen, I., Yli-Juuti, T., Gagné, S., Asmi, E., Aalto, P., Petäjä,
560 T., Kerminen, V.-M., and Kulmala, M.: Charged and total particle formation and growth rates
561 during EUCAARI 2007 campaign in Hyytiälä, Atmospheric Chemistry and Physics, 9, 4077-
562 4089, 2009.

563 Manninen, H., Nieminen, T., Asmi, E., Gagné, S., Häkkinen, S., Lehtipalo, K., Aalto, P.,
564 Vana, M., Mirme, A., and Mirme, S.: EUCAARI ion spectrometer measurements at 12
565 European sites–analysis of new particle formation events, Atmospheric Chemistry and
566 Physics, 10, 7907-7927, 2010.
567 Manninen, H., Franchin, A., Schobesberger, S., Hirsikko, A., Hakala, J., Skromulis, A.,
568 Kangasluoma, J., Ehn, M., Junninen, H., and Mirme, A.: Characterisation of corona-
569 generated ions used in a Neutral cluster and Air Ion Spectrometer (NAIS), Atmospheric
570 Measurement Techniques, 4, 2767, 2011.
571 Manninen, H. E., Mirme, S., Mirme, A., Petäjä, T., and Kulmala, M.: How to reliably detect
572 molecular clusters and nucleation mode particles with Neutral cluster and Air Ion
573 Spectrometer (NAIS), Atmos. Meas. Tech. Discuss, 2016.
574 Mazon, S. B., Kontkanen, J., Manninen, H. E., Nieminen, T., Kerminen, V.-M., and Kulmala,
575 M.: A long-term comparison of nighttime cluster events and daytime ion formation in a
576 boreal forest, Boreal Environment Research, 2016.
577 Mirme, S., and Mirme, A.: The mathematical principles and design of the NAIS-a
578 spectrometer for the measurement of cluster ion and nanometer aerosol size distributions,
579 Atmospheric Measurement Techniques, 6, 1061, 2013.
580 Pierce, J., Westervelt, D., Atwood, S., Barnes, E., and Leaitch, W.: New-particle formation,
581 growth and climate-relevant particle production in Egbert, Canada: analysis from 1 year of
582 size-distribution observations, Atmospheric Chemistry and Physics, 14, 8647-8663, 2014.
583 Pushpawela, B., Jayaratne, R., and Morawska, L.: Temporal distribution and other
584 characteristics of new particle formation events in an urban environment, Environmental
585 Pollution, 233, 552-560, https://doi.org/10.1016/j.envpol.2017.10.102, 2018.
586 Rose, C., Sellegri, K., Asmi, E., Hervo, M., Freney, E., Colomb, A., Junninen, H., Duplissy,
587 J., Sipilä, M., and Kontkanen, J.: Major contribution of neutral clusters to new particle

588 formation at the interface between the boundary layer and the free troposphere, Atmospheric
589 Chemistry and Physics, 15, 3413-3428, 2015.
590 Russell, L., Mensah, A., Fischer, E., Sive, B., Varner, R., Keene, W., Stutz, J., and Pszenny,
591 A.: Nanoparticle growth following photochemical α-and β-pinene oxidation at Appledore
592 Island during International Consortium for Research on Transport and
593 Transformation/Chemistry of Halogens at the Isles of Shoals 2004, Journal of Geophysical
594 Research: Atmospheres, 112, 2007.
595 Salimi, F., Rahman, M., Clifford, S., Ristovski, Z., and Morawska, L.: Nocturnal new particle
596 formation events in urban environments, Atmospheric Chemistry and Physics, 17, 521-530,
597 2017.
598 Salma, I., Borsós, T., Weidinger, T., Aalto, P., Hussein, T., Dal Maso, M., and Kulmala, M.:
599 Production, growth and properties of ultrafine atmospheric aerosol particles in an urban
600 environment, Atmospheric Chemistry and Physics, 11, 1339, 2011.
601 Smith, J., Dunn, M., VanReken, T., Iida, K., Stolzenburg, M., McMurry, P., and Huey, L.:
602 Chemical composition of atmospheric nanoparticles formed from nucleation in Tecamac,
603 Mexico: Evidence for an important role for organic species in nanoparticle growth,
604 Geophysical Research Letters, 35, 2008.
605 Stolzenburg, M. R., McMurry, P. H., Sakurai, H., Smith, J. N., Mauldin, R. L., Eisele, F. L.,
606 and Clement, C. F.: Growth rates of freshly nucleated atmospheric particles in Atlanta,
607 Journal of Geophysical Research: Atmospheres, 110, 2005.
608 Suni, T., Kulmala, M., Hirsikko, A., Bergman, T., Laakso, L., Aalto, P., Leuning, R., Cleugh,
609 H., Zegelin, S., and Hughes, D.: Formation and characteristics of ions and charged aerosol
610 particles in a native Australian Eucalypt forest, Atmospheric Chemistry and Physics, 8, 129-
611 139, 2008.

612 Svenningsson, B., Arneth, A., Hayward, S., Holst, T., Massling, A., Swietlicki, E., Hirsikko,
613 A., Junninen, H., Riipinen, I., and Vana, M.: Aerosol particle formation events and analysis
614 of high growth rates observed above a subarctic wetland–forest mosaic, Tellus B, 60, 353-
615 364, 2008.
616 Winkler, P.: The growth of atmospheric aerosol particles with relative humidity, Physica
617 Scripta, 37, 223, 1988.
618 Wise, M. E., Semeniuk, T. A., Bruintjes, R., Martin, S. T., Russell, L. M., and Buseck, P. R.:
619 Hygroscopic behavior of NaCl-bearing natural aerosol particles using environmental
620 transmission electron microscopy, Journal of Geophysical Research: Atmospheres, 112,
621 2007.
622 Yli-Juuti, T., Riipinen, I., Aalto, P. P., Nieminen, T., Maenhaut, W., Janssens, I. A., Claeys,
623 M., Salma, I., Ocskay, R., and Hoffer, A.: Characteristics of new particle formation events
624 and cluster ions at K-puszta, Hungary, Boreal Environment Research, 14, 683-698, 2009.
625 Yli-Juuti, T., Nieminen, T., Hirsikko, A., Aalto, P., Asmi, E., Hõrrak, U., Manninen, H.,
626 Patokoski, J., Maso, M. D., and Petäjä, T.: Growth rates of nucleation mode particles in
627 Hyytiälä during 2003− 2009: variation with particle size, season, data analysis method and
628 ambient conditions, Atmospheric Chemistry and Physics, 11, 12865-12886, 2011.
629 Zhang, Q., Stanier, C. O., Canagaratna, M. R., Jayne, J. T., Worsnop, D. R., Pandis, S. N.,
630 and Jimenez, J. L.: Insights into the chemistry of new particle formation and growth events in
631 Pittsburgh based on aerosol mass spectrometry, Environmental science & technology, 38,
632 4797-4809, 2004.

633

634

Figures

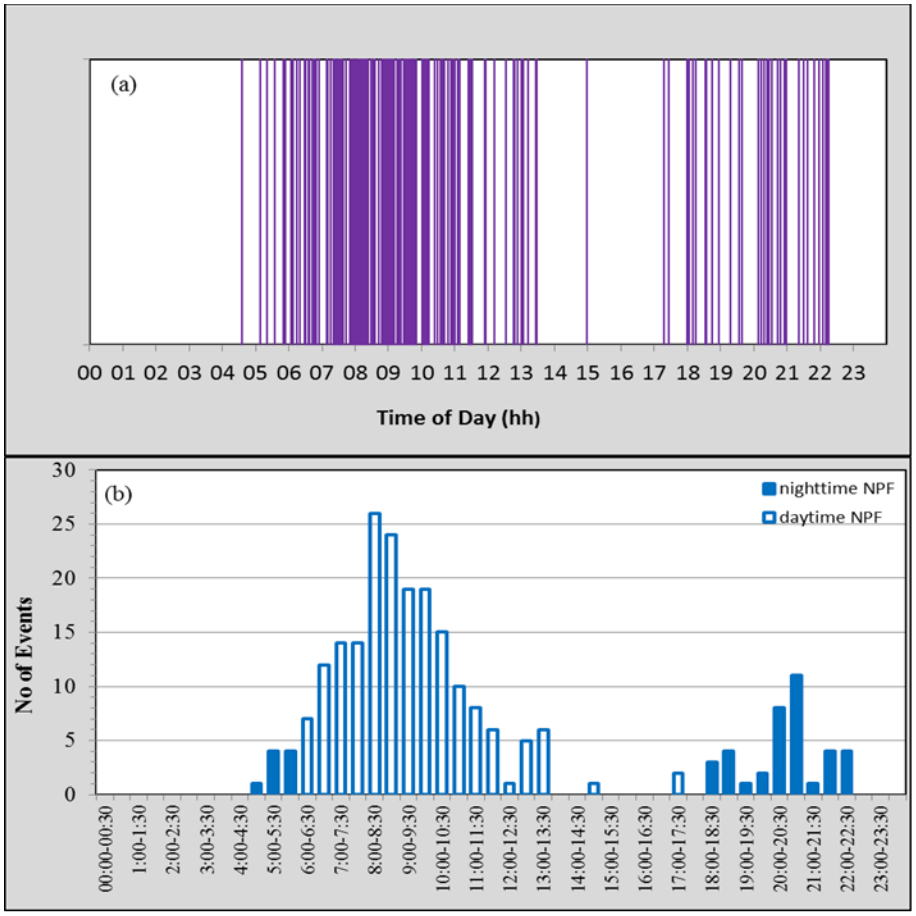

Figure 1: (a) Summary of starting times of all NPF events and (b) histogram for the number of events

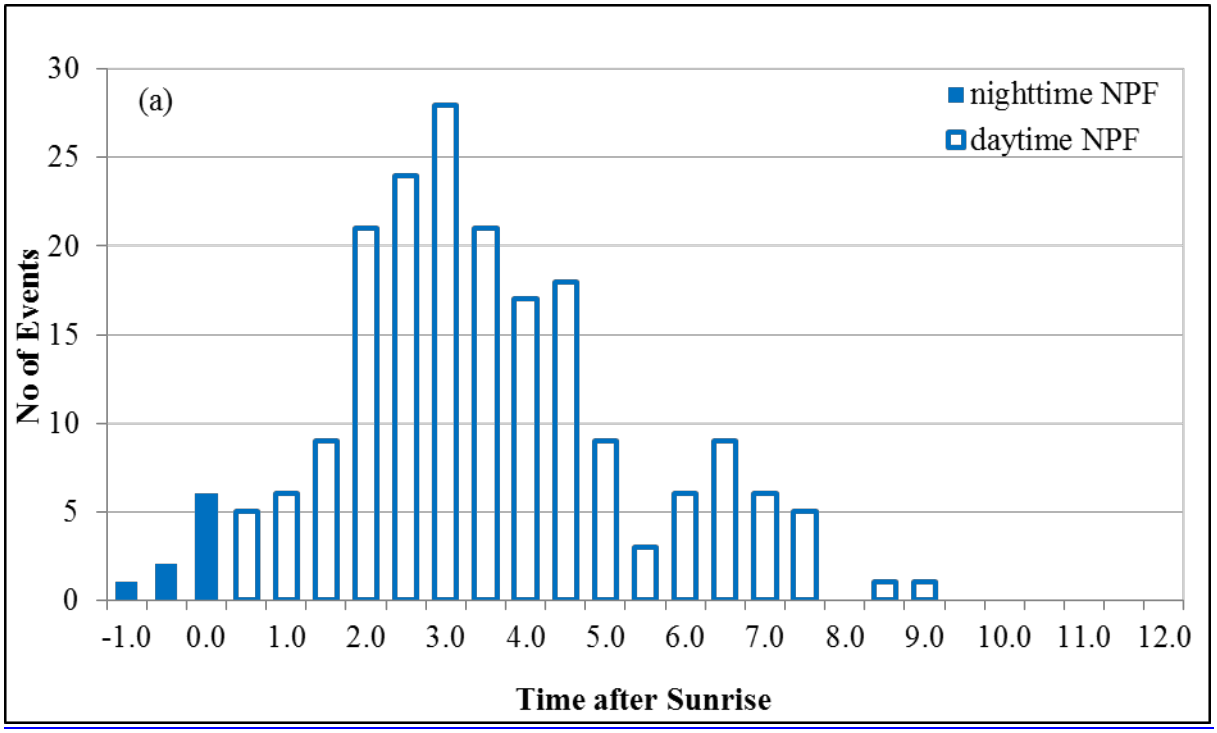

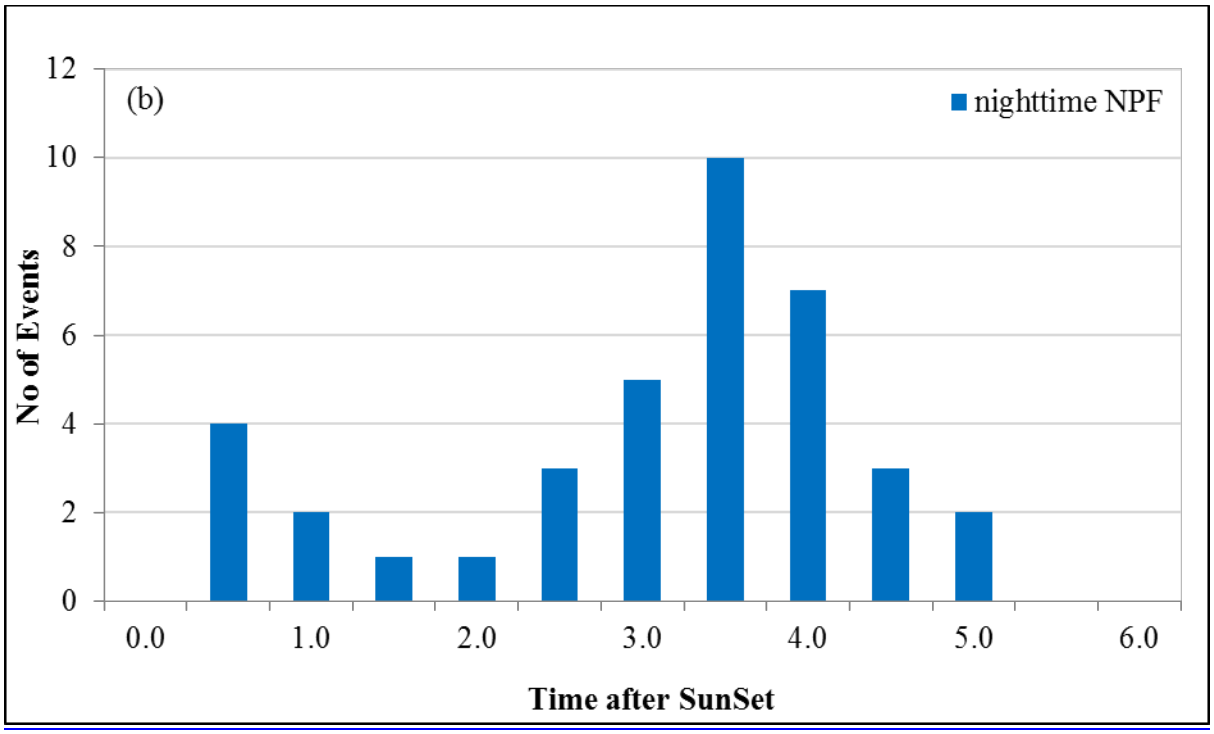

Figure 1: Distribution of start times of daytime NPF events as a function of time after sunrise (a) nighttime NPF events as a function of time after sunset (b). In figure 1 (a) the three bars on the extreme left correspond to times before sunrise.

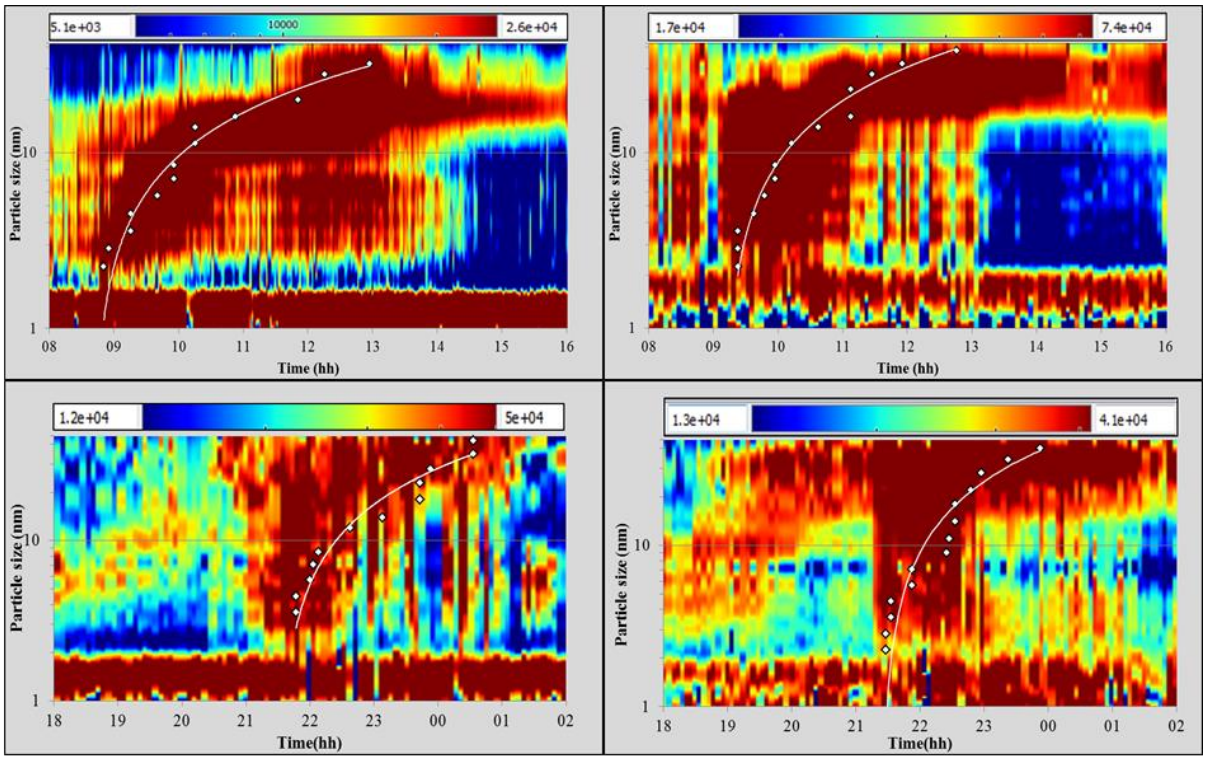
5.1e+03
10000
2.6e+04
1.7e+04
7.4e+04
1.2e+04
5e+04
1.3e+04
4.1e+04
Particle size (nm)
Time (hh)
Time(hh)

646

647

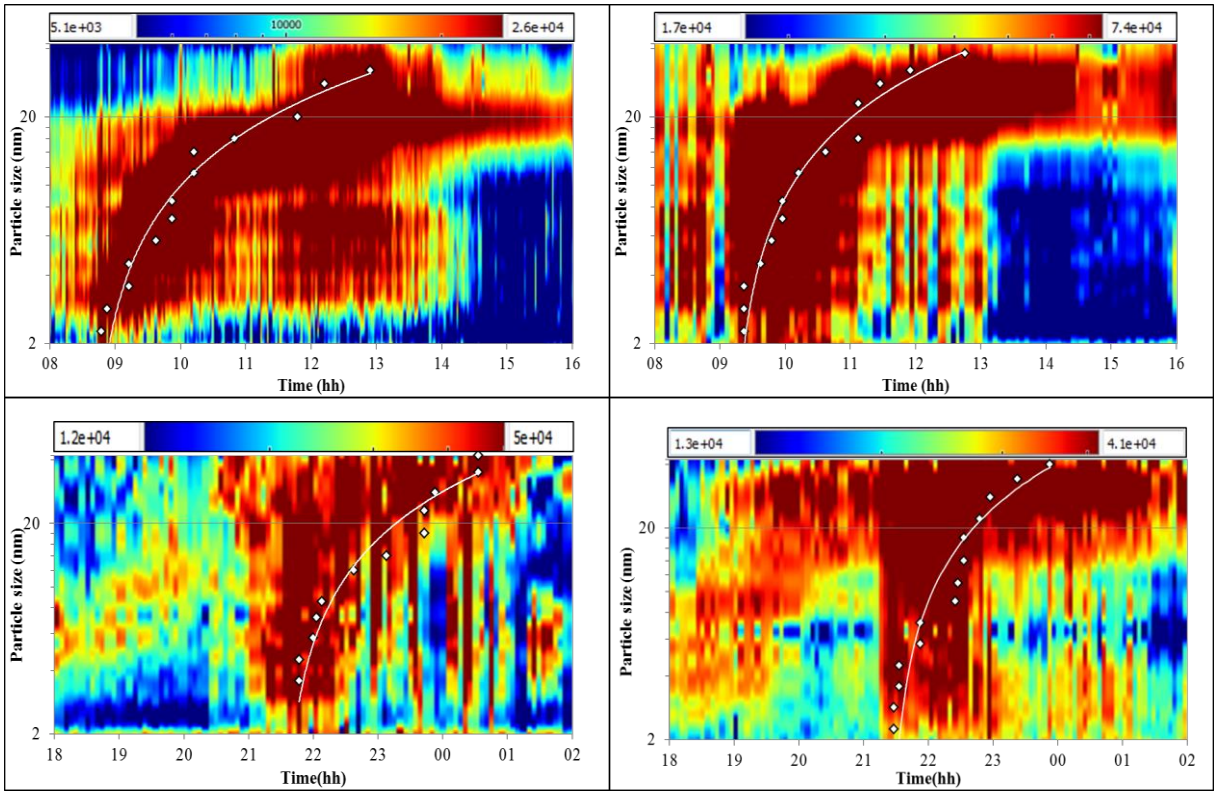
5.1e+03
10000
2.6e+04
1.7e+04
7.4e+04
1.2e+04
5e+04
1.3e+04
4.1e+04
Particle size (nm)
Time (hh)
Time(hh)

648

Figure 2: NAIS spectragrams of the daytime NPF events (upper panel) and nighttime NPF (lower panel). The colour contour represents the PNC and the markers represent the times at which the PNC reached its maximum value at each particle size. The unit of PNC is per cubic centimetre. ~~Data below 2 nm should be treated with caution due to instrumentation limitations as described in the text.~~

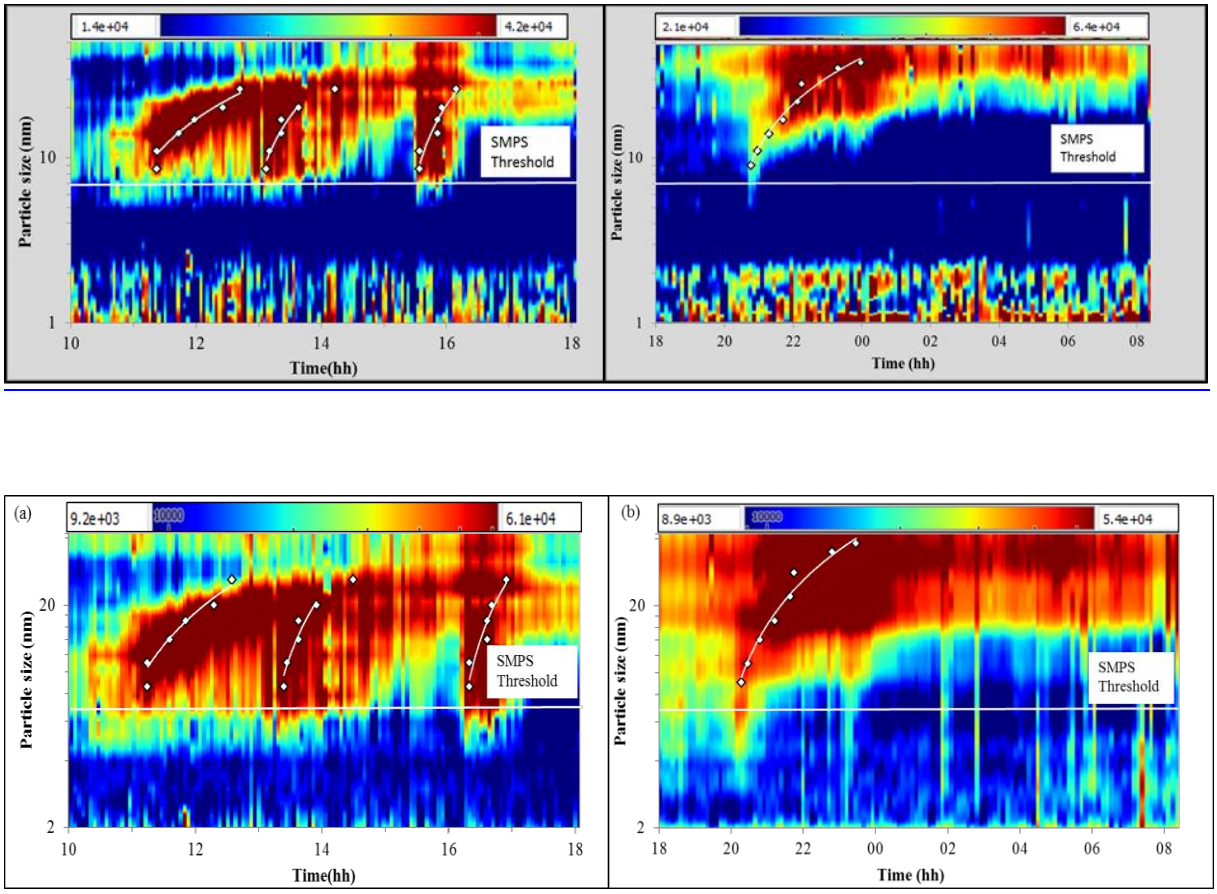

Figure 3: NAIS spectragrams of the growth events that occurred during (a) day time (b) night time. Note the "floating banana" shape which indicates that these are clearly not NPF events. The SMPS cannot detect particles at sizes below the horizontal white line. The colour contour represents the PNC and the markers represent the times at which the PNC reached its maximum value at each particle size. The unit of PNC is per cubic centimetre.

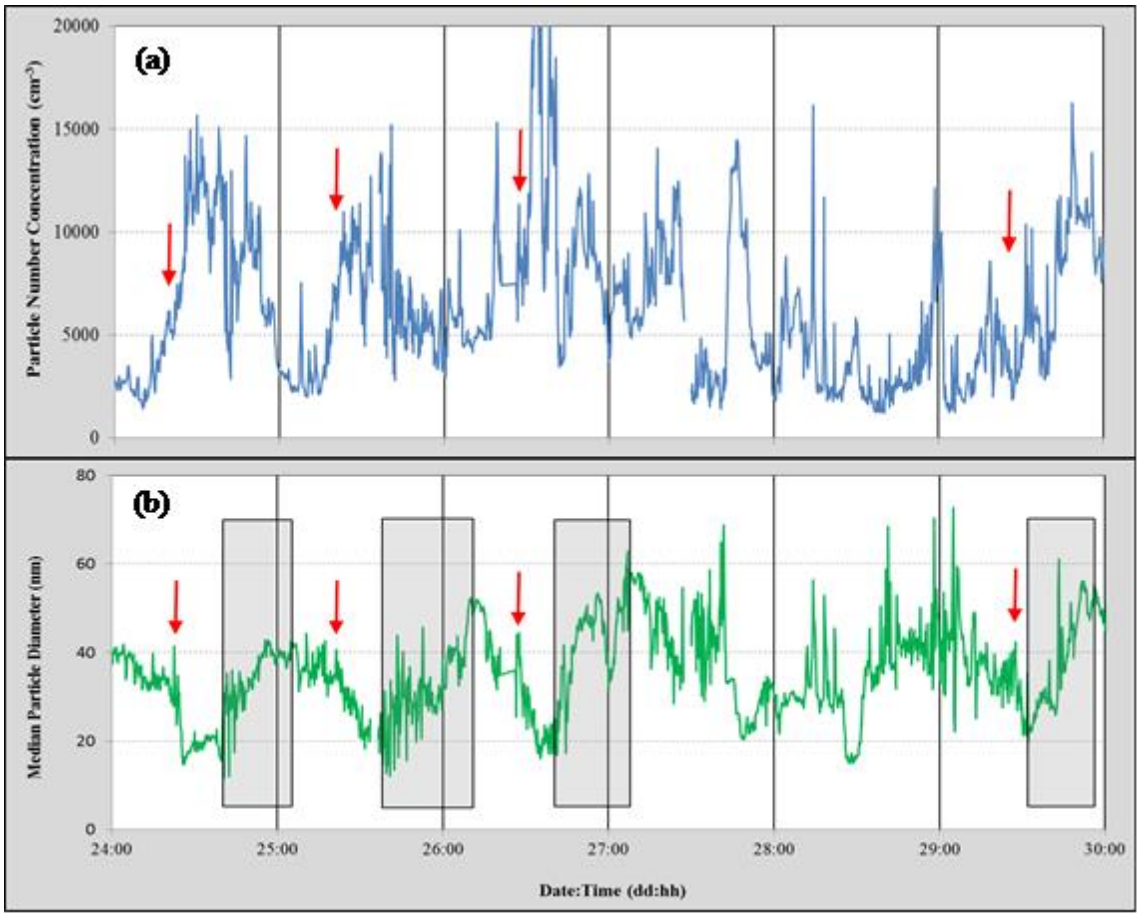
(a)
Particle Number Concentration (cm-3)
20000
15000
10000
5000
0
(b)
Median Particle Diameter (nm)
80
60
40
20
0
24:00
25:00
26:00
27:00
28:00
29:00
30:00
Date:Time (dd:hh)

690

691

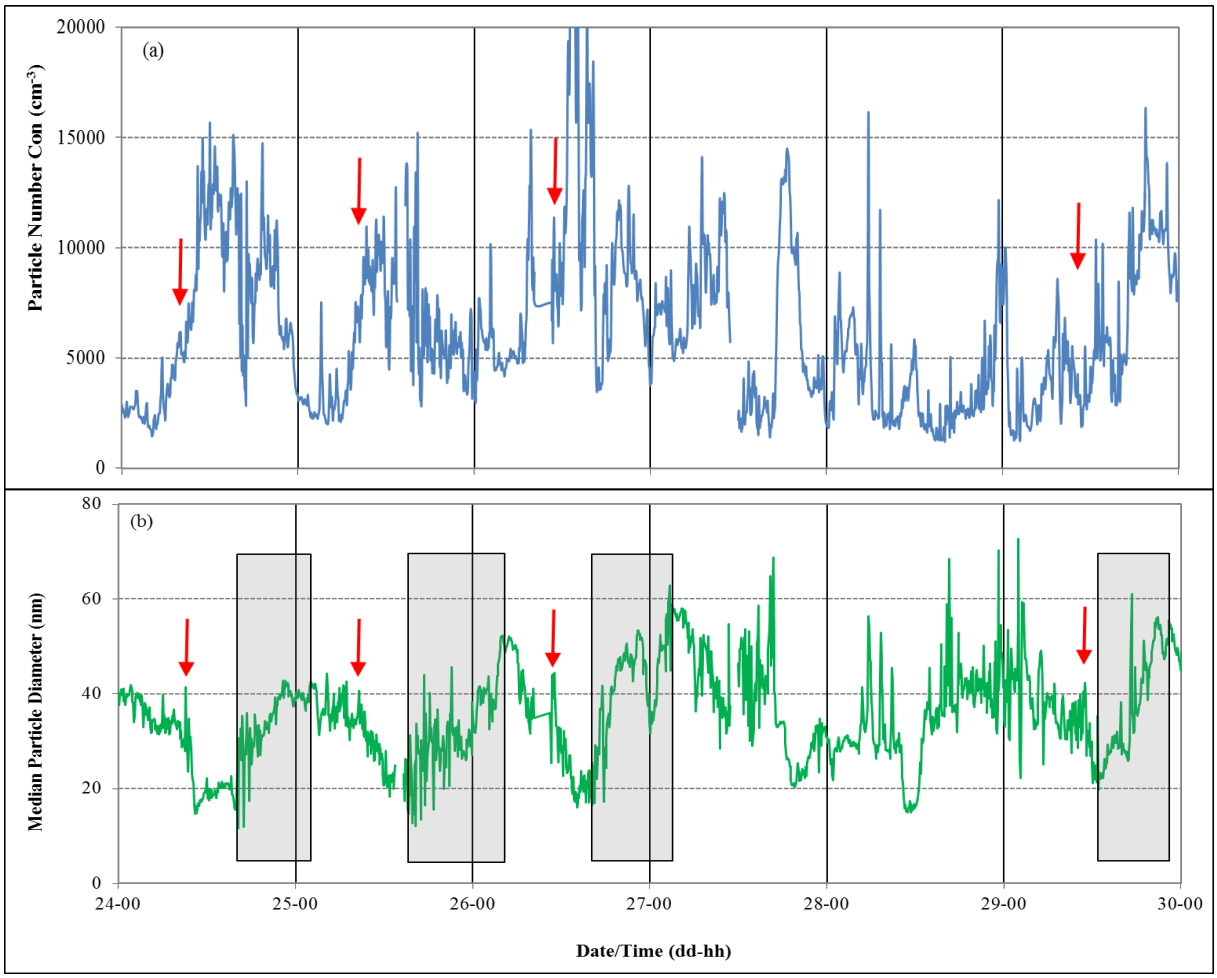

Figure 4: (a) the total PNC and (b) median particle diameter from the SMPS during 24 July-30 July, 2012. Red arrows and gray boxes represent the day time NPF events and the growth events, respectively.

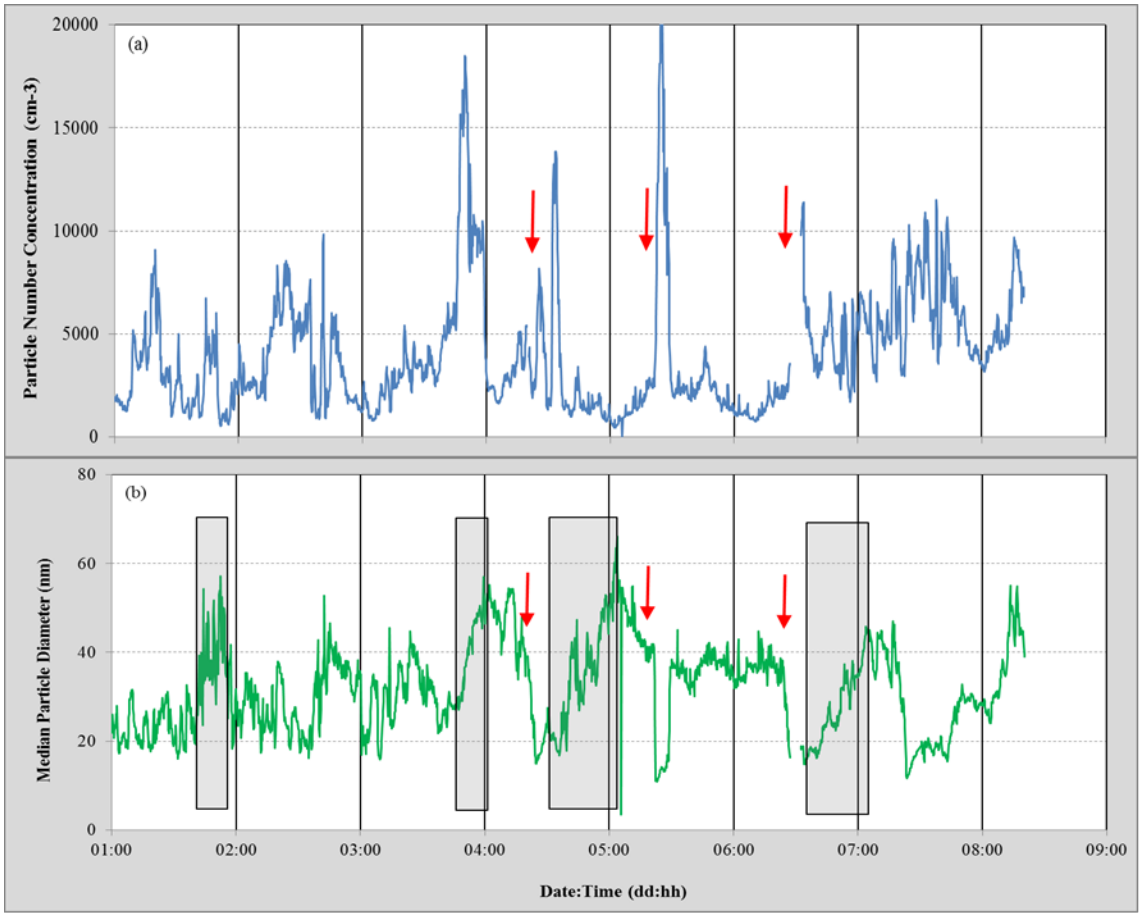
(a)
Particle Number Concentration (cm-3)
20000
15000
10000
5000
0
(b)
Median Particle Diameter (nm)
80
60
40
20
0
01:00
02:00
03:00
04:00
05:00
06:00
07:00
08:00
09:00
Date:Time (dd:hh)

701

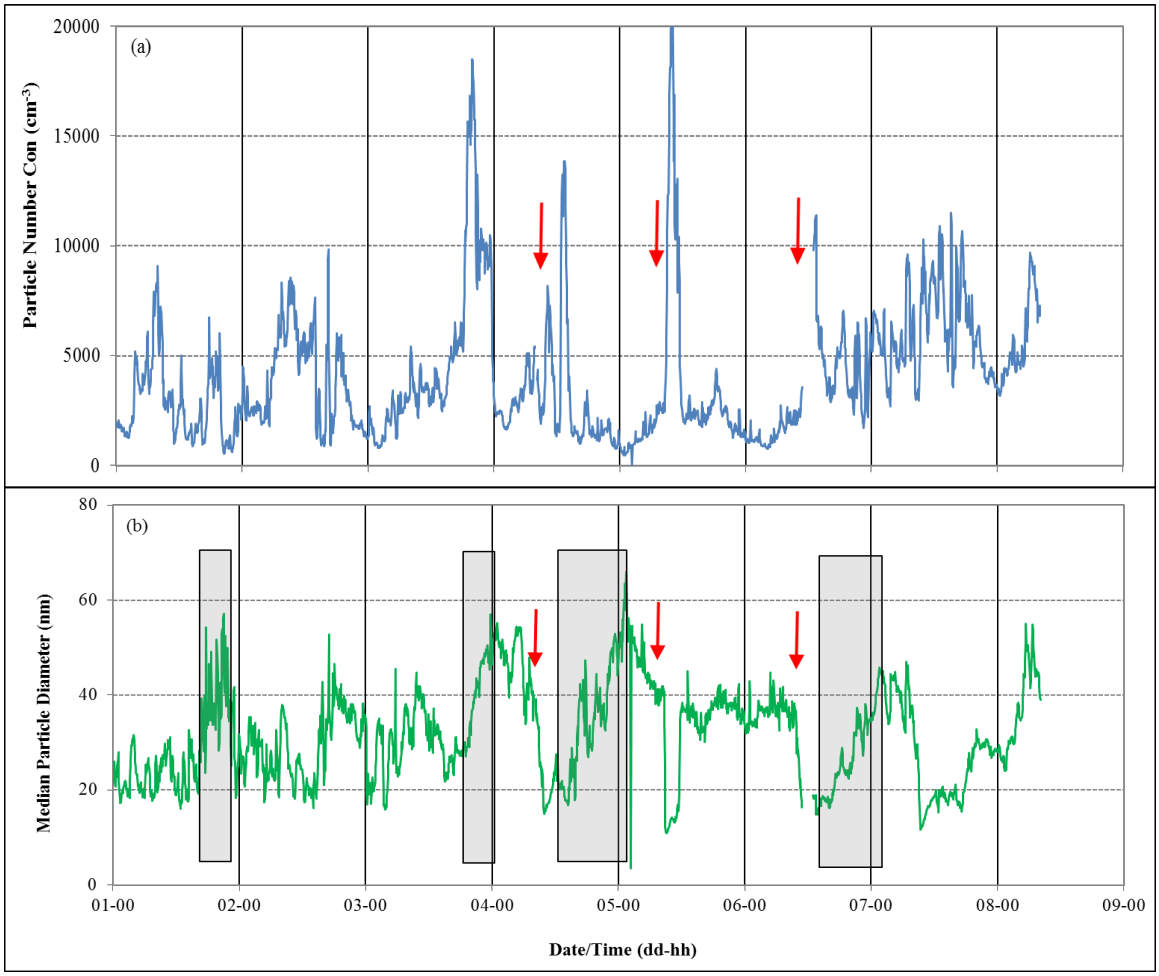

Figure 5: (a) the total PNC and (b) median particle diameter from the SMPS during 1 June-7 June, 2012. Red arrows and gray boxes represent the daytime NPF events and the growth events, respectively.

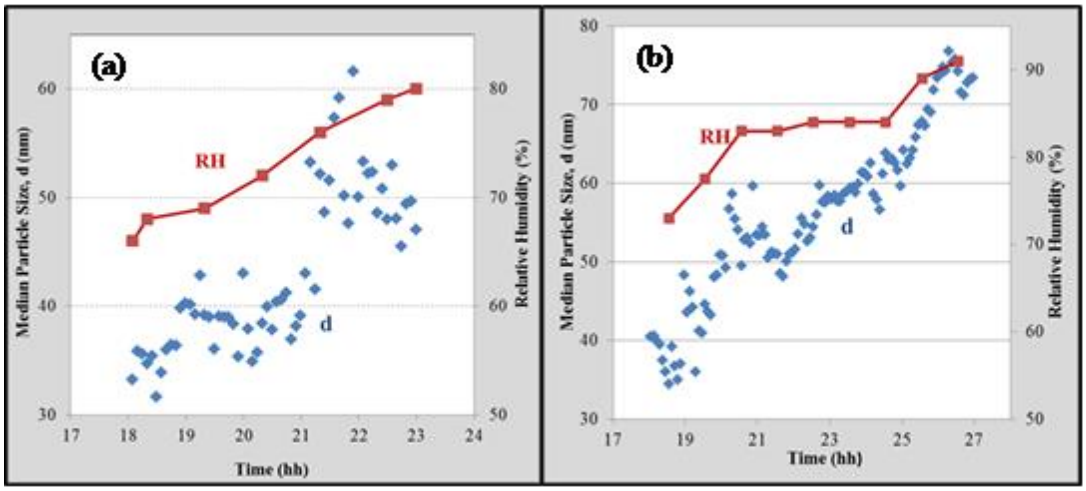

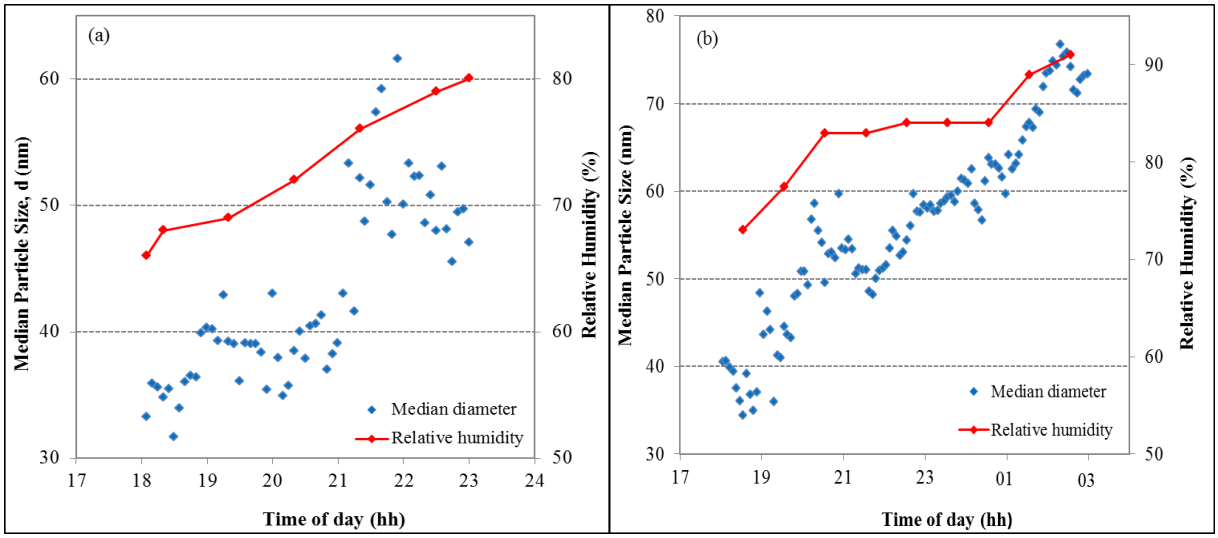

Figure 6: Median particle size and relative humidity as a function of time for growth events on July 16 and July 20, 2012, respectively

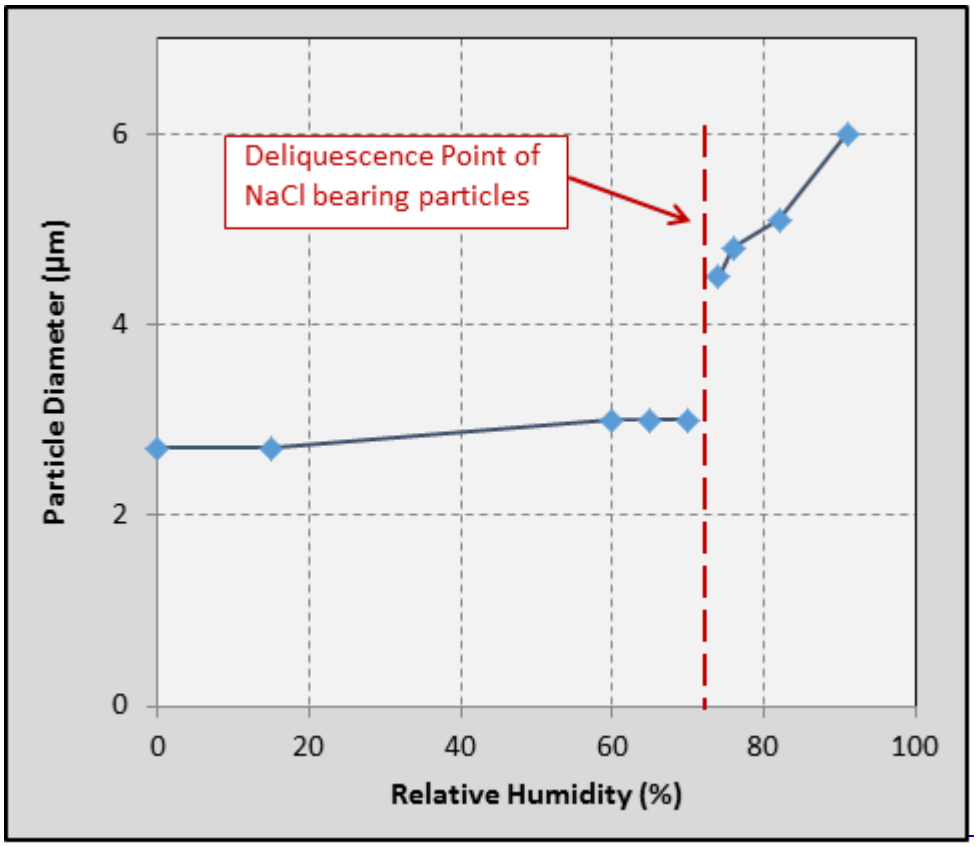

Figure 7: Particle diameter as a function of relative humidity for NaCl-bearing particles. The figure is plotted using the data presented in Wise et al. (2007).

735 **Table 1: Summary of studies reporting night time NPF events**

736 SMPS: Scanning mobility particle sizer, AIS: Air ion spectrometer, BSMA: Balanced

737 scanning mobility analyser, FMPS: Fast mobility particle sizer

Study	Location	Occurrence rate		Instrument (size range)
		Day time	Night time	
Svenningsson et al. (2008)	Abisko, Sweden (characterized by Subartic birch forest)	46/195 days (23%)	31/195 days (16%)	SMPS (10-500 nm) AIS (0.4-40 nm)
Junninen et al. (2008)	Pine Forest, Hyytiala, Finland		344/1279 days (27%)	BSMA (0.4-6.3nm) AIS (0.34-40 nm)
Suni et al. (2008)	Eucalypt forest, Tumbarumba, Australia	184/351 days (52%)	112/351days (32%)	AIS (0.34-40 nm)
Kalivitis et al. (2012)	Finokalia, Lassithiou, Greece (remote coastal site)	53/365 days (15%)	39/365 days (11%)	SMPS (9-900 nm) AIS (0.8-42 nm)
Man et al. (2015)	Suburban coastal site, Hong Kong	12/112 days (11%)	5/112 days (4%)	FMPS (5.6-560 nm)
Mazon et al. (2016)	SMEAR II, boreal forest, Hyytiala, Finland		using neg ions: 1324/4015 days (34%) using pos ions: 1172 /4015 days (30%)	BSMA (0.8-8 nm)
Salimi et al. (2017)	25 sites across Brisbane (characterized by urban environment)	146/285 days (51%)	73/285 days (26%)	SMPS (9-414 nm)
Kammer et al. (2017)	Landes forest, France	2/16 days (12.5%)	6/16 days (37.5%)	SMPS (10-478 nm)

738

739

740 Table 2: Summary of the day time and night time NPF events

741

Year	Total Data Available Days	Strong NPF events			Weak NPF events			Total NPF events		
		Day time	Night time	Total	Day time	Night time	Total	Day time	Night time	Total
2012	253	97	7	104	9	9	18	106	16	122
2015	65	18	4	22	5	7	12	23	11	34
2017	167	44	7	51	16	13	29	60	20	80
Total Events		159	18	177	30	29	59	189	47	236
Total days	485	159	18	177	30	29	59	181	47	213
Occurrence rate (%)		33	4	37	6	6	12	37	10	44

742

743

744

745

746

747

748

749

750

751

752

753

754

755

756

757

758

759

760 Table 3: The mean and the range of meteorology and gas phase parameters on NPF and non-

761 event days

Parameter	Winter Months NPF days	Winter Months non-event days	Summer Months NPF days	Summer Months non-event days	NPF days	non-event days
			Meteorology			
Solar radiation (W m^{-2})	346 (230-490)	316 (95-476)	600 (202-818)	476 (68-818)	505 (202-818)	397 (68-818)
Temperature (^{0}C)	17 (12-19)	16 (12-25)	24 (18-29)	24 (19-32)	21 (12-29)	20 (12-32)
Relative Humidity (%)	59 (31-73)	70 (27-90)	52 (23-73)	63 (25-86)	54 (23-73)	66 (25-90)
Wind direction (^{o})	215 S-SW	203 S-SW	197 S-SW	177 S-SW	205 S-SW	200 S-SW
Wind Speed ($m\ s^{-1}$)	1.07 (0.3-3.1)	1.17 (0.3-3.6)	1.60 (0.3-4.7)	2.25 (0.3-5.8)	1.40 (0.3-4.7)	1.72 (0.3-5.8)
			Gas Phase			
Visibility (Mm^{-1})	15 (6-42)	34 (2-112)	19 (7-41)	29 (6-114)	18 (6-42)	31 (2-114)
Ozone (ppb)	12 (1-29)	10 (2-26)	20 (1-32)	19 (3-35)	17 (1-32)	15 (2-35)
SO_2 (ppb)	7 (6-10)	6 (1-9)	5 (1-14)	3 (1-9)	6 (1-14)	5 (1-9)

762

763

764

765

766

767

768 Table 4: Summary of the growth events, which did not follow the NPF events, obtained using

769 the NAIS data.

Year	Total Data Available Days	Growth Events		
		Day time	Night time	Total
2012	253	24	59	83
2015	65	4	21	25
2017	167	26	55	81
Total events		54	135	189
Total days	485	54	135	179
Occurrence rate (%)		11	28	37

770

771

772

773

774